POSSIBLE INVOLVEMENT OF MYOSIN IN MALARIA DEVELOPMENT AND INVASION

USAWADEE SAKULKHU

A THESIS SUBMITTED IN PARTIAL FULFILLMENT
OF THE REQUIREMENTS FOR
THE DEGREE OF MASTER OF SCIENCE (BIOCHEMISTRY)
FACULTY OF GRADUATE STUDIES
MAHIDOL UNIVERSITY
2004

ISBN 947-04-4454-7

POSSIBLE INVOLVEMENT OF MYOSIN IN MALARIA DEVELOPMENT AND INVASION

Usawadee Sakulkhu
.....
Miss Usawadee Sakulkhu
Candidate

.....
Assist.Prof.Rutaiwan Tohtong,
Ph.D.(Molecular Genetics)
Major-advisor

Prapon W-lairat
.....
Prof.Prapon Wilairat,
Ph.D.(Biochemistry)
Co-advisor

Ramm Hoon
.....
Assoc.Prof.Rassmidara Hoonsawat,
Ph.D.
Dean
Faculty of Graduate Studies

Prapon W-lairat
.....
Prof.Prapon Wilairat,
Ph.D.(Biochemistry)
Chair
Master of Science Programme
in Biochemistry
Faculty of Science

POSSIBLE INVOLVEMENT OF MYOSIN IN MALARIA DEVELOPMENT AND INVASION

was submitted to the Faculty of Graduate Studies, Mahidol University
for the degree of Master of Science (Biochemistry)
on
June 7, 2004

Usawadee Sakulkhu
.....
Miss Usawadee Sakulkhu
Candidate

.....
Assist.Prof.Rutaiwan Tohtong,
Ph.D.(Molecular Genetics)
Chair

Prapon Wilairat
.....
Prof.Prapon Wilairat,
Ph.D.(Biochemistry)
Thesis Defense Committee

Peerapan Tan-ariya
.....
Prof.Peerapan Tan-ariya,
Ph.D.(Microbiology)
Thesis Defense Committee

Rassm Hoon
.....
Assoc.Prof.Rassmidara Hoonsawat,
Ph.D.
Dean
Faculty of Graduate Studies
Mahidol University

Prasert Sobhon
.....
Prof.Prasert Sobhon,
Ph.D.
Dean
Faculty of Science
Mahidol University

ACKNOWLEDGEMENTS

I have spent much time to complete my work and along the way to the end of This, I have been given many help from many people who have worked with and supported me very much to make this thesis possible.

I would like to express my sincere gratitude to Assistant Professor Rutaiwan Tohtong, my major advisor, for her valuable advice, her understanding and also for her care and cncouragement throughout the study.

I would like to express my deepest appreciation to Professor Prapon Wilairat, my co-advisor, who always kindly gave expert guidance, continuous support, and also for his care, understanding and encouragement throughout the study.

My grateful appreciation is also expressed to Professor Peerapan Tan-ariya, who was the external examiner of the thesis defense, for her kindness constructive training in determining malaria parasite morphology, and for providing suggestions for improvement of the thesis.

My special thanks are extended to Miss Anong Kitjaroentham, Miss Nongluk Srivilaijaroen and Miss Napawan Ponmee who always give me good help and suggestions not only for experiments but also other aspects. I would especially like to thank to all members of Pr.315 and Pr.311 for their good care to make me warm and happy. My thanks are also expressed to members of Pr.303, R303/1 and members of Biochemistry Department for their help, friendship and sincerity. I also gratefully thank to Miss. Mayurachat Poopha and Mrs. Poonsook Puang-reor for their help in preparation of malaria parasite culture materials.

Finally, I would like to express my deepest gratitude to my Dad, Mom and my younger sisters for their infinite love, and giving their best that are always in my mind. I am grateful to my grandparents for their care and love. My sincere gratitude is also expressed to Assistant Professor Damnurn Vachirodom for financial support.

Usawadee Sakulkhu

POSSIBLE INVOLVEMENT OF MYOSIN IN MALARIA DEVELOPMENT AND INVASION

USAWADEE SAKULKHU 4336153 SCBC/M

M.Sc. (BIOCHEMISTRY)

THESIS ADVISORS: RUTAIWAN TOHTONG, Ph.D.(MOLECULAR GENETICS), PRAPON WILAIRAT, Ph.D. (BIOCHEMISTRY)

ABSTRACT

Growth of asexual blood stages of the malaria parasite occurs in the erythrocyte. The malaria parasite passes through a series of distinctive stages of development, from ring form to trophozoite form, and then undergoes division into schizonts to give rise to a cluster of merzoites, which upon rupture of erythrocyte, are released into the blood stream to invade other uninfected erythrocytes to start a new cycle of development. The intracellular parasite causes changes to erythrocyte shape and deformability, which is controlled by myosin II, whose function is in turn regulated by myosin light chain kinase (MLCK) and myosin ATPase. *Plasmodium falciparum* myosin has been reported to be involved in invasion. The involvement of myosin in malaria development and invasion were assessed by using ML-7, MLCK inhibitor and BDM, myosin ATPase inhibitor. By employing ^{3}H-hypoxanthine incorporation assay, ML-7 and BDM inhibited development of *P. falciparum* K1 strain from ring to schizont stage with IC_{50} of 6.3±1.1 μM and 6.4±1.1 mM, respectively. I further assessed which particular stage of development was affected by the inhibitors by determining parasitemia under a microscope. BDM was effective in inhibiting all intraerythrocytic stages of parasite development and at the invasion step as well, whereas ML-7 was more effective at inhibiting development from ring to trophozoite stage. When the two drugs were tested in combination, sub-inhibitory concentrations of BDM did not affect ML-7 activity, and sub-inhibitory concentrations of ML-7 did not change the IC_{50} of BDM. Taken altogether, these findings indicated that myosin activity is required for malaria parasite intraerythrocytic development and invasion, but the contribution of host and parasite myosins to these processes remained unresolved.

KEY WORDS: MALARIA / ERYTHROCYTE / MYOSIN / DEVELOPMENT / INVASION

87 pp. ISBN 974-04-4454-7

บทบาทของ myosin ต่อการเจริญเติบโตและการบุกรุกเข้าสู่เม็ดเลือดแดงของเชื้อมาลาเรีย
(POSSIBLE INVOLVEMENT OF MYOSIN IN MALARIA DEVELOPMENT AND INVASION)

อุษาวดี สกุลคู 4336153 SCBC/M

วท.ม. (ชีวเคมี)

คณะกรรมการควบคุมวิทยานิพนธ์: ฤทัยวรรณ โต๊ะทอง, Ph.D. (MOLECULARGENETICS), ประพนธ์ วิไลรัตน์, Ph.D. (BIOCHEMISTRY)

บทคัดย่อ

การเจริญเติบโตของเชื้อมาลาเรียในระยะไม่อาศัยเพศเกิดขึ้นในเม็ดเลือดแดง โดยเชื้อมาลาเรียจะพัฒนาจากระยะวงแหวนไปสู่ระยะโทรโฟซอยต์จากนั้นเชื้อจะพัฒนาเข้าสู่ระยะไชซอนต์โดยนิวเคลียสของโทรโฟซอยต์แบ่งตัวเพิ่มจำนวนขึ้น ในที่สุดเชื้อมาลาเรีย (ระยะเมอโรซอยต์) จะแตกออกจากเม็ดเลือดแดงและบุกรุกเข้าสู่เม็ดเลือดแดงใหม่ เพื่อเจริญเติบโตในวัฏจักรใหม่ต่อไป การเจริญเติบโตของเชื้อมาลาเรียในเม็ดเลือดแดงทำให้เกิดการเปลี่ยนแปลงรูปร่างของเม็ดเลือดแดงซึ่งถูกควบคุมโดย myosin II โปรตีนชนิดนี้ถูกควบคุมโดยเอนไซม์ myosin light chain kinase (MLCK) และ myosin ATPase มีรายงานการศึกษาพบว่าโปรตีน myosin ของ *Plasmodium falciparum* เกี่ยวข้องกับกระบวนการบุกรุกเข้าสู่เม็ดเลือดแดง ในการวิจัยครั้งนี้มุ่งศึกษาบทบาทของ myosin ต่อพัฒนาการและการบุกรุกเข้าสู่เม็ดเลือดแดงโดยใช้ ML-7 ซึ่งเป็นตัวยับยั้งการทำงานของ MLCK และ BDM ซึ่งเป็นตัวยับยั้งการทำงานของ myosin ATPase โดยการใช้ ^{3}H-hypoxanthine incorporation assay จากการศึกษาพบว่า ML-7 และ BDM สามารถยับยั้งการเจริญเติบโตของ *P.falciparum* K1 strainได้ 50% ที่ความเข้มข้น 6.3 ±1.1 μM และ 6.4 ±1.1 mM ตามลำดับ นอกจากนั้นได้ทำการศึกษาเพิ่มเติมถึงผลกระทบของตัวยับยั้งต่อการพัฒนาของเชื้อในแต่ละระยะภายใต้กล้องจุลทรรศน์ ผลการศึกษาแสดงให้เห็นว่า BDM สามารถยับยั้งพัฒนาการของเชื้อในทุกระยะรวมถึงการบุกรุกเข้าสู่เม็ดเลือดแดงด้วย ในขณะที่ ML-7 สามารถยังยั้งพัฒนาการของเชื้อจากระยะวงแหวนสู่ระยะโทรโฟซอยต์ได้มากกว่าระยะอื่นๆ เมื่อใช้ตัวยับยั้งสองชนิดรวมกันพบว่า BDM ที่ความเข้มข้นต่ำ ไม่มีผลต่อประสิทธิภาพการยับยั้งการเจริญเติบโตของเชื้อของ ML-7 และ ML-7 ที่ความเข้มข้นต่ำไม่มีผลต่อประสิทธิภาพการยับยั้งการเจริญเติบโตของเชื้อของ BDM ด้วยเช่นกัน ผลจากการวิจัยในครั้งนี้ชี้บ่งว่าการทำงานของ myosin จำเป็นต่อการเจริญเติบโตและการบุกรุกเข้าสู่เม็ดเลือดแดง แต่บทบาท myosin ของเชื้อมาลาเรียและของเม็ดเลือดแดงในกระบวนการเหล่านี้ยังไม่สามารถหาคำอธิบายที่แน่ชัดได้

87 หน้า ISBN 974-04-4454-7

CONTENTS

CONTENTS (cont.)

CONTENTS (cont.)

CONTENTS (cont.)

LIST OF TABLES

LIST OF FIGURES

LIST OF FIGURES (cont.)

ABBREVIATIONS

ABPs	actin binding proteins
AMA1	apical merozoite antigen-1
ATP	adenosine-5'-triphosphate
^{o}C	degree Celcius
D	Aspartic acid
DNA	deoxyribonucleic acid
DW	distilled water
E	Glutamic acid
EBA175	erythrocyte binding antigen 175 kDa
ELC	myosin essential light chain
ER	endoplasmic recticulum
F-actin	filamentous actin
FIC	fractional inhibitory concentration
f-MAST	*falciparum* merozoite assenmblage of subpellicular microtubule
g	gram
G-actin	globular actin
h	hour
ICM	incomplete medium
IC_{50}	50% inhibitory concentration
i.e.	id. Est (latin), that is
Ki	inhibitory constant
kDa	kilodalton
MCP1	merozoite capping protein-1
MHC	myosin heavy chain
MLCK	myosin light chain kinase
MSP-1	merozoite surface protein-1

ABBREVIATIONS (cont.)

min	minute
ml	milliliter
mM	millimolar
µl	microliter
µM	micromolar
PM	parasite membrane
PV	parasitophorous vacuole
PVM	parasitophorous vacuole membrane
%	percentage
RLC	myosin regulatory light chain
S	Serine
SD	standard deviation
sec	second
SEM	standard error of the mean
T	Threonine
TVN	tubovesicular network
v/v	volume by volume

CHAPTER 1
INTRODUCTION

Malaria remains one of the most widespread parasitic diseases. There are estimated 300-500 million clinical cases annually and 1.5 to 2.7 million people die each year, mainly of children under 5 year olds. Countries in tropical Africa are estimated to have more than 80% of all clinical cases and more than 90% of all parasite carriers. In 1990, 75%of all recorded malaria cases, excluding the Africa region, was concentrated in 9 countries: India, Brazil, Afghanistan, Sri Lanka, Thailand, Indonesia, Vietnam, Cambodia and China. In Thailand, the highest incidence continues to be recorded in Trat (bordering Cambodia) and Tak (bordering Myanmar), Chantaburi and Kanchanaburi (1-5).

Efforts to control malaria are becoming decreasingly successful because of antimalarial drug resistance in the parasite, insecticide resistance in mosquitoes, and socio-economic deficits and warfare in human population (6). There is also slow progress in development of malarial vaccine (7, 8). So chemotherapy control of malaria caused by *Plasmodium falciparum* is a major goal.

1.1 Malaria life cycle

The genus *Plasmodium* is eukaryotic protozoan in phylum Apicomplexa; class: Sporozoa; subclass: Coccidia; order: Eucoccidia; suborder: Haemosporina. More than 100 species of the genus *Plasmodium* are found in the blood of reptiles, birds and mammals. Of these, four species, *Plasmodium falciparum*, *Plasmodium vivax*, *Plasmodium ovale*, and *Plasmodium malariae*, cause malaria in human.

Infected female *Anopheles* mosquito transmits malaria to human via biting during bloodmeal.

The biology of the four species of *Plasmodium* is generally similar and consists of two phases: sexual and asexual. The asexual stages develop in human, first

in the liver and then in the circulating erythrocytes; the sexual stages develop in the mosquito (Figure 1).

1.1.1 Sexual stages

Differentiation of the parasites into male and female gametocytes (the sexual stages) occurs in vertebrate host. They are the principal stages responsible for continued transmission of parasites from one host to another via a complex sexual life cycle in the mosquito vector. When ingested by female mosquitoes, mature circulating forms of the sexual stages undergo a rapid process (10-20 min) of gametogenesis, resulting in the formation of male and female gametes. One female gamete (macrogamete) emerges from one female gametocyte. Male gametocyte initiates exflagellation which is a process in which one male gametocyte has three mitotic division cycles to give eight active sperm-like microgametes. Fertilization by one exflagellated form of microgametes and macrogamete produces zygote (the only diploid stage). The zygote develops into a motile diploid ookinete which penetrates the gut epithelial cells and come to lie under the basement membrane. The parasites then transform into oocysts within 24 hours of ingestion of the blood meal. The parasites undergo rapid meiotic division to obtain more than 1,000 haploid sporozoites from one oocyst. They mature within 10-14 days, escape from oocyst, and invade the salivary gland and await introduction into a host during blood feeding (9, 10).

1.1.2 Asexual stages

During female *Anopheles* mosquitoes blood feeding, saliva fluid is injected into the wound to initiate the infection. A small 10-15 μm, spindle-shaped, motile form called sporozoite is injected into subcutaneous tissue and less frequently directly into the bloodstream, from there, the parasite travels to the liver within an hour. After the sporozoites enter liver cells, they begin exoerythrocytic development.

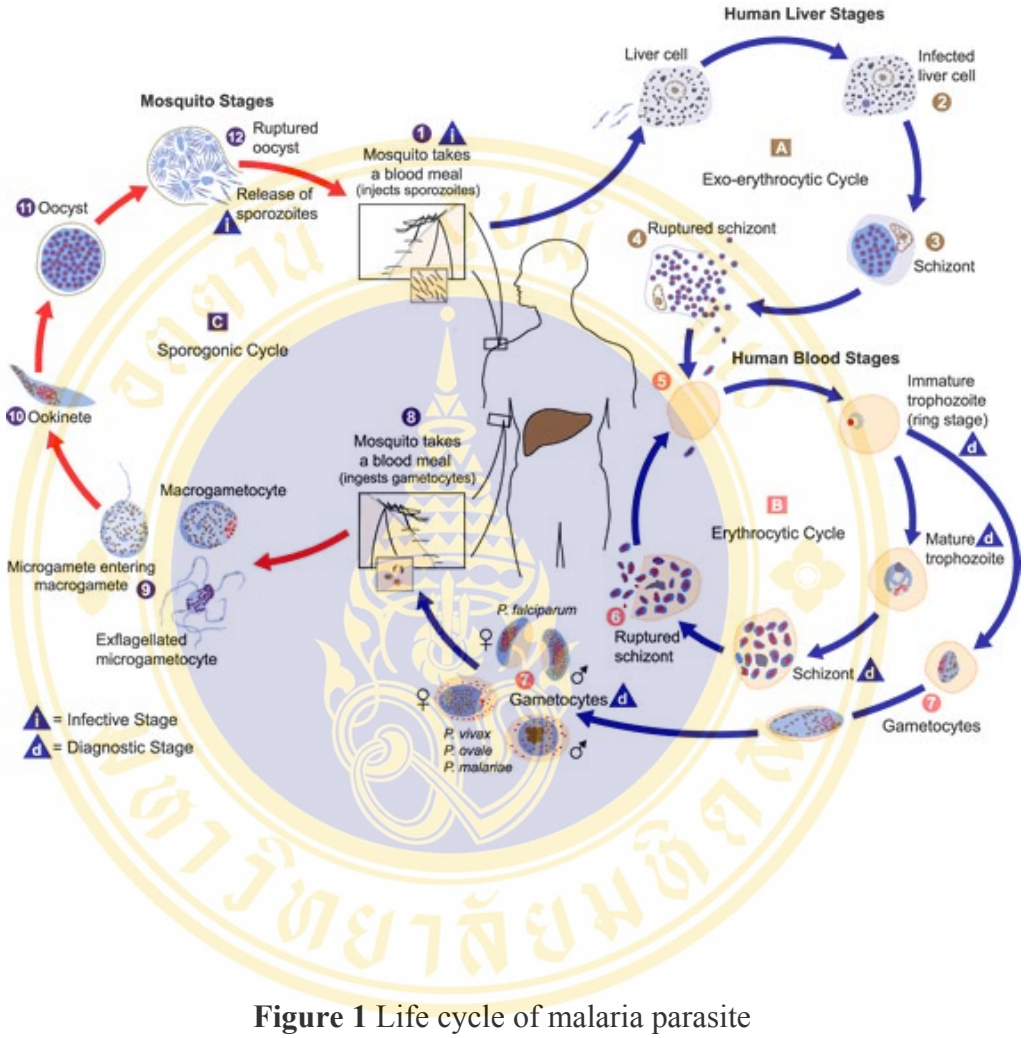

Figure 1 Life cycle of malaria parasite
(http://www.cdc.gov/malaria/biology/life_cycle.html)

1.1.2.1 Exoerythrocytic cycle

Within one hour, the sporozoites eventually reach the parenchymal cells of the liver. The route sporozoites follow to the liver has not been definitely established. *In vitro* studies with the rodent malaria *P. berghei* suggest that circulating sporozoites are first taken up by the Kuffer cells and from there pass into hepatocytes. Multiple rounds of cell invasion through hepatocytes prior to infect their target cells induces the exocytosis of sporozoite apical organelles, a prerequisite for infection with formation of a vacuole which appear to be necessary to potentiate the intracellular survival of malaria sporozoites within liver hepatocyte (11, 12). Inside the liver cell, the parasites undergo asexual division, the exoerythrocytic schizogony. The number of merozoites produced within each infected cell and length of this exoerythrocytic phase are individual characteristics of each species of *Plasmodium*. *P. falciparum* can mature within 5-7 days and each of its sporozoite produces 40,000 merozoites; 6-8 days, and about 1,000 merozoite for *P. vivax*; 9 days, 15,000 for *P. ovale*; 12-16 days and 2,000 merozoites for *P. malariae*.

Some of species of malarial parasite (e.g. *P. vivax* and *P. ovale*) have a phenomenon of relapse (the reappearance of parasitemia in sporozoite-induced infection following adequate blood schizonticidal therapy). Exoerythrocytic form of relapsing malaria persist in the liver as a result of cyclic development, i.e., rupture of infected hepatocytic cells and invasion of new red cells. There are some experimental evidences that support a different hypothesis for the mechanisms of the relapse. It holds that some sporozoites fail to initiate immediate exoerythrocytic development in the liver and remain latent, as the so-called hypnozoites, capable of delayed development and initiation of relapse. *P. falciparum* and *P. malariae* do not develop hypnozoites and therefore lack the capacity to relapse.

1.1.2.2 Intraerythrocytic stage (13)

When merozoites are relased from the liver schizonts, they invade erythrocytes and initiate the erythrocytic phase of infection.

The merozoite stage

The invasive merozoite stage of the parasite is important immunologically because it is briefly extracellular and thus expose to host antibodies between leaving one erythrocyte and entering the next. The merozoite is 1.6 μm, oval shape, with a low, flat-ended projection (the apical prominence) at one end. Each merozoite contains all the equipment needed to escape from its host erythrocyte, finds and attaches to a fresh one, invade it, and rapidly restarts feeding. Underneath the merozoite plasma membrane, attached to it by filamentous cross-bridges, lie two more outer and inner vesicle of a flattened membranous sac or cisterna (also sometimes termed an alveola), the three together forming the pellicle. Under the plasma membrane of the apical prominence, there are three dense proteinaceous rings (polar rings) to which are anchored the apical border of the pellicular cisterna and a longitudinally running band of subpellicular microtubules. The merozoite is composed of the apical organelles: the rhoptries, micronemes and dense granules which all are membranous vesicle that discharge their contents during invasion and change the shape and composition of the membrane of the invaded erythrocyte. The rhoptries are twin pear-shaped, 650 nm long, their narrow ends (ducts) converging on the apical prominence. Micronemes are 120 x 40 nm organelle; they cluster around the rhoptry ducts. The secretion of micronemes and rhoptries might be vital both to the attachment of the merozoite apex to an erythrocyte, and to subsequent formation in the erythrocyte surface of an invasion pit, which eventually envelopes the merozoite in a parasitophorous vacuole (PV). The dense granules are rounded bodies lying separately within the apical cytoplasm of merzoite. Protein in dense granules are involved in increasing PV membrane (PVM) area, and presumably facilitating the change in shape of the parasite to ring stage. The merozoite also contains cyotskeleton which plays important role in invasion process. The microtubules are called f-MAST (falciparum merozoite assemblage of subpellicular microtubules). Antimicrotubule have been found to inhibit erythrocyte invasion. Actins are also present, including G-and F-actin. A merozoites specific myosin (Pfmyo-A) has been immunolocalized to the plasma membrane and is likely to be part of an acto-myosin motor responsible for propelling the merozoite into the erythrocyte during invasion. These various cytoskeletal

elements are dismantled when the merozite has entered the erythrocyte. The surface of the merozoite is coated with many proteins. The best candidate is the merozoite surface protein (MSP) 1 complex, comprising the most abundant proteins of the merozoite exterior, and is known to be cleaved and, in most part, shed during invasion.

The ring stage

After invasion, the parasite flattens into a thin discoidal, flat or cup-shaped ring form of the trophozoite stage. Typically, this has a thick rim of cytoplasm housing the major organelles – nucleus, mitochondrion, plastid, most of the ribosomes and endoplasmic reticulum (ER) – while the center of the disc is thin and contains few structures. Because of the thickened perimeter of the cell and the position of the nucleus, Giemsa-stained films viewed under the light microscope show the parasite as a ring like structure, giving this stage its name. During the ring and early trophozoite stage, genes associated with the cytoplasmic transcriptional and translational machinery, glycolysis and ribonucleotide biosynthesis are induced (14). The parasite begins to feed on the surrounding erythrocyte through a small, dense ring at the surface of the parasite, the cytostome. The cytostome possesses a double-membrane containing of the outer membrane (PM) and inner membrane (PVM). Through this intriguing structure are pulled small portions of erythrocyte cytosol, with neighboring areas of parasitophorous vacuole membrane (PVM) and PM of the parasite, which are then pinched off and digested within vacuoles in the interior of the parasite. The parasite uses host haemoglobin as a source of amino acids. However, they can not degrade the haemoglobin haem byproduct. Free haem is potentially toxic to parasite. Therefore, during haemoglobin degradation most of the liberated haem is crystallized into brown haemozoin (malaria pigment), which is stored within food vacuoles throughout the erythrocytic phase of the life cycle. Initially there are several small vacuoles, some perhaps derived from endocytosis not confined to the cytostome, but in later stages, these usually fuse to form a single large pigment vacuole. As the parasite grows, the area of the PVM surrounding it also increases. The ring stage is surrounded by PVM which contain two distinct types of intraerythrocytic structure. The first are the Maurer's clefts, which appear as flattened lamellar membranes with a

unique set of parasite protiens. The second are membrane loops of varying size called tubovesicular network (TVN) that contain parasite encoded protein distinct from those of cleft. The exact relationship between Maurer's clefts and TVN are not known (15). The ring eventually changes shape to a more rounded or irregular trophozoite.

Trophozoite stage

Distinction between the ring and trophozoite stages depends on cell size and shape rather than any fundamental internal difference, and indeed the ring is more properly called the ring form of the trophozoite stage. Both feed on the erythrocyte and gradually alter it by exporting various parasite proteins into its cytoplasm and to its surface. The numbers of free ribosomes multiply greatly, and the ER enlarges, both changes denoting increased protein synthesis. During trophozoite and early schizont stage, the expression of the deoxyribonucleotide biosynthesis is concomitant with the induction of DNA replication machinery transctripts, reflecting a tight relationship between DNA synthesis and production of precursor for this process (14).

The surface area of the trophozoite now enlarges greatly, with the formation at its surface of irregular bulges and deep tubular invaginations. Some of the bulges extend out into the erythrocyte cytosol as thin veil-like structures. Some of these configurations reach the underside of the RBC membrane, but no certain instances of fusion to form an opening on to its surface have been discovered. These various membranous structures are called Maurer's clefts. By the mid-trophozoite stage, the rough ER has proliferated considerably, and the putative Golgi complex has increased in size and complexity. Some of the proteins are incorporated into the growing area of the PVM but others traverse this barrier to pass as dense aggregates, often associated with Maurer's clefts, through the erythrocyte cytosol to its surface, where they bind to the erythrocyte cytoskeleton and membrane. Some of these proteins produce small angular elevations (knobs) on the erythrocyte surface causing erythrocytes infected with more mature stages to become even less deformable than ring forms (16). EM and fluorescence imaging have visualized some of these events, and suggest that different proteins might have different trafficking

routes, some of which do not involve a traditional Golgi complex. The knobs are responsible for the sequestration of trophozoites and schizonts (and perhaps late rings) in deep visceral blood vessels, and give rise to the pathogenic obstruction of placental and cerebral vasculature.

The schizont

Technically speaking, a schizont is an intraerythrocytic parasite that is undergoing or has undergone replicative nuclear division. However, the synthesis of some of the molecules needed for parasite multiplication, including DNA, is known to start in the trophozoite stage. Conversely, trophic ingestion of erythrocyte cytosol lasts until quite late in the schizont period, almost totally depleting the haemoglobin while adding further haemozoin crystals to the pigment vacuole, which then becomes compacted into a single, dense, rounded mass. In a similar manner, export of parasite proteins into the erythrocyte continues until late in the life of the schizont. The surface of the erythrocyte often becomes quite angular in profile, as the exported parasite proteins distort the cytoskeleton and membrane of the cell, in addition to increasing the numbers of knobs at its surface, as clearly shown by recent atomic-force scanning microscopy (17). The nucleus divides about four times, cell divisions probably alternating with bouts of DNA synthesis to produce about 16 nuclei, although as many as 20 are often found in singly infected erythrocyte. Nuclear division is endomitotic, a common feature in unicellular eukaryotes, and the segregating chromosomes and spindle apparatus remain within the nuclear envelope throughout the process. In the phase of schizont development at the eight-nucleus stage, the individual nuclei move towards the surface of the parasite, with the spindles orientated tangential to the perimeter of the cell. Nuclear division is accompanied by numerous cytoplasmic changes that prefigure merozoite formation, and there is a great proliferation of rough ER and free ribosomes throughout the parasite. This phase is followed by creation of a series of centres of merozoite formation, in which the various elements of merozoites are assembled, beginning with the apical organelles. Merozoite cytoskeletal components, including polar rings and microtubules, are assembled beneath the merozoite surface and a cleavage furrow now forms around each nascent merozoite, defining its shape. Before complete separation,

a nucleus, mitochondrion and plastid move into each merozoite from the central area of schizont cytoplasm and the merozoite coat is, in some as yet undefined manner, added to its surface. Finally, the PVM and erythrocyte membranes are breached, an event that is probably triggered by apical organelle secretions from the merozoites. In merozoite release process, treatment of E64 a cysteine protease inhibitor shows that merozoites enclosed within the PVM first exit from the host erythrocyte and then rapidly escape from the PVM by a proteolysis-dependent mechanism (18). The parasites are now ready to find and exploit new erythrocytes.

1.1.2.3 Host cell invasion

Invasion of erythrocytes by merozoite unfolds in four steps: (1) initial recognition and attachment of the merozoite loosely to the erythrocyte membrane; (2) reorientation and junction formation between the apical end of the merozoite and the release of rhoptry-microneme substances with vacuole formation; (3) movement of the junction and invagination of the erythrocyte membrane around the merozoite accompanied by removal of the merozoite's surface coat, and finally (4) resealing of the parasitophorous vacuole membrane and erythrocyte membrane after completion of merozoite invasion (as shown in Figure 2 (10)).

The initial attachment of the merzoites to the erythrocyte surface is random and reversible. Attachment is followed by an apparently organized motile event, the reorientation of parasite to bring its apical prominence into contact with the host. After apical orientation, there is a tight interaction of parasite receptors with specific ligands on the erythrocyte membrane. The relative important of the roles played in this process by merozoite coat proteins (eg. merozoite surface protein 1 (MSP1)) or apically secreted components (eg. apical merozoite antigen1 (AMA1), erythrocyte-binding antigen 175kDa (EBA175)) remains unclear; antibodies against appropriate determinants of numerous merozoite proteins will block invasion. Merozoite capping protein 1(MCP1) has been uniquely identified at the tight junction.

During invasion, MCP1 moves from the apical end around to posterior of the merozoite, suggesting a role for this protein in facilitating attachment or movement of the junction along the parasite surface coat. The merozoite

secrete material from their rhoptries, engendering local vacuolation of the erythrocyte membrane. The merozoite moves into the deepening invaginate, while the electron-dense junction travels as an annulus over its surface. The membrane of this invagination eventually seals at the posterior end of the merozoite to form the PVM. The PVM is probably a product both the secretions of the rhoptries and of the host cell membrane lipid bilayer, augmented soon after invasion by the discharge of the dense bodies into the PV (19).

Cytoskeletal and motor protein in merzoite motility (20)

These are composed of the following.

1. Actin

There are two actin genes in *P. falciparum*: *pf-actinI* is expressed throughout the life cycle, and *pf-actinII* is expressed only in sexual stages. F-actin polymers are double helical filaments capable of extension or shortening at either end, which are remodelled and regulated by actin binding protein (ABPs). Capping and uncapping of actin could provide the mechanism for localized actin filament growth to generate movement of the merozoites into the host cell. A role for actin in merozoite invasion suggested by the blocking action of cytochalasin B.

2. Microtubules

P. faciparum microtubules are abundant in mitotic spindles in schizont. Subpellicular microtubules are found in sporozoites, gametocytes, ookinetes and merozoite. In merozoite, it consists of two (sometimes three) microtubules, rumming in parallel along one side of the merozoite from the third polar ring towards the posterior. This structure is called *P. falciparum* merozoite assemblage of subpellicular microtubules (f-MAST). Shortening the f-MAST by antimicroctubule drugs (Colchicine which prevents further tubulin polymerization and, at high

concentration, depolymerizes microtobules, and dinitroanilines which disassemble microtubule) reduce the number of resultant ring. Taxol which promotes polymerization and stabilizes microtubules, did not inhibit invasion (21). These suggested that the integrity of the f-MAST is important, but that invasion does not require dynamic microtubule. In addition, f-MAST may act as a directional guide, indicating the apical polarity of merozoite. Kinesins and dyneins have been identified in *P. falciparum* genome and are also present in merozoite. So f-MAST role might be involved in microtubule-based motor in organelle and protein trafficking (20).

3. Myosin

Pfmyo-A is *P. falciparum* myosin, which is now thought to play role in merozoite entry into erythrocyte. Pfmyo-A is present in the right place and at the right time to be a component of the merozoite invasion motor. It is expressed essentially only in mature merozoite and located predominance towards the apex. Electronmicroscopy indicates that it is located between the parasite membrane and cisternal membrane. It is not detected in young ring stage, and its first appearance is in the schizont (22).

However, it has not been known that how the motor is control. There is a model of *P. falciparum* merozoite invasion showing some possible relationships between structure and events in invasion (20). The authors have modeled both the carriage of merozoite constituents on microfilaments and the flow of membrane forward, while myosin is anchored at attachment site. As described earlier, F-actin are short double-helical filaments. Ubiquitination might also regulate the polymerization state of actin. Capping and uncapping of actin could provide the mechanism for localized actin filament growth. Regulation of Pfmyo-A activity might involve a mechanism similar to ameoeboid yeast myosin I which is regulated by phosphorylation at a concensus site, the TEDS site. The TEDS site of Pfmyo-A is a threonine residue, capable of phosphorylation. In this model, the authors suggested linkage via G-protein from surface receptor. Pfmyo-A lack the long tail and their tails can instead bind to other structures, such as membrane vesicle or organelle (see Figure 3).

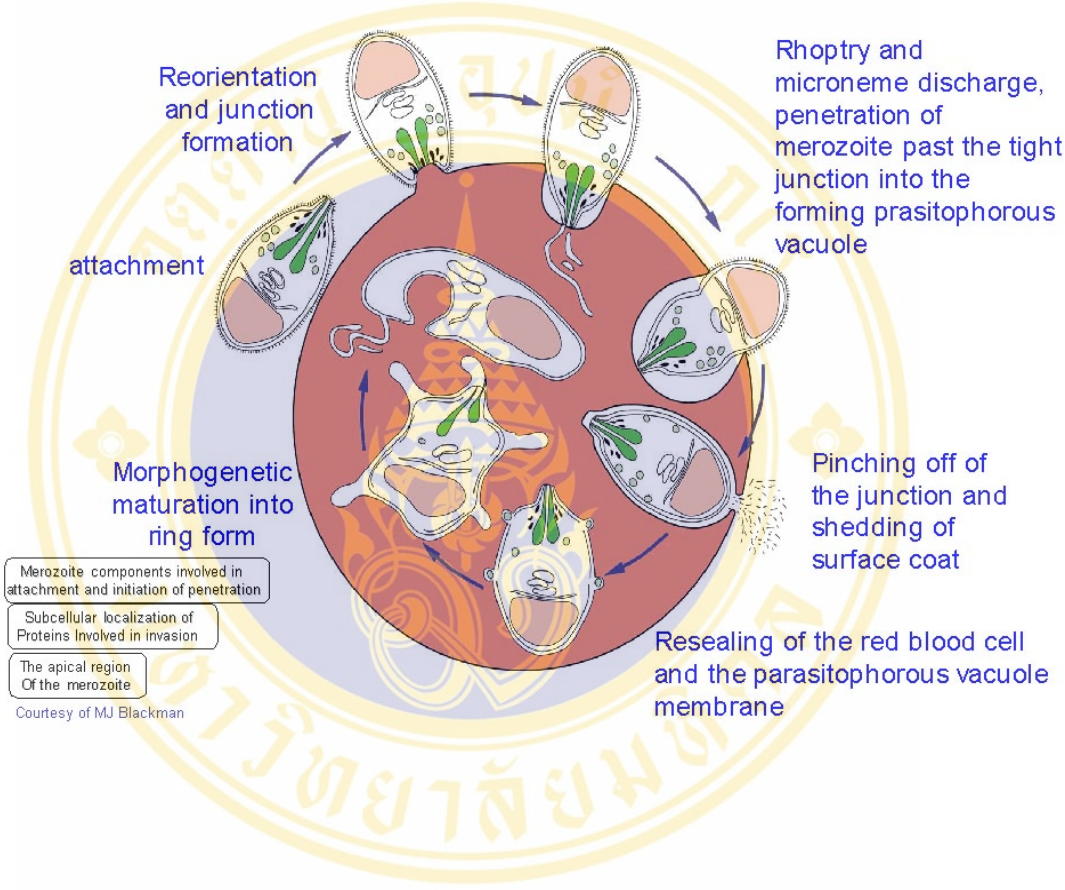

Figure 2 Malaria parasite invasion

(http://sites.huji.ac.il/malaria/invasion.html)

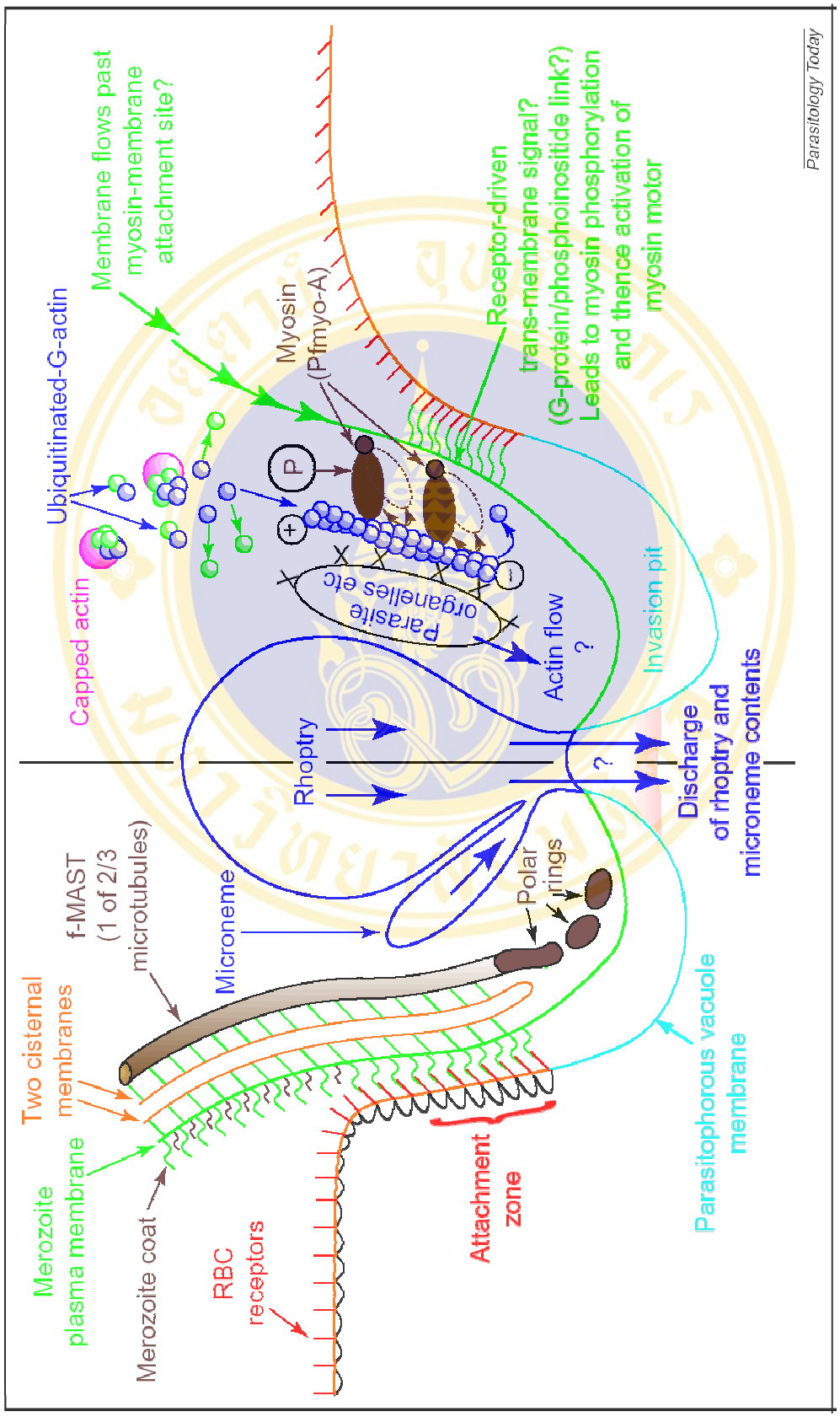

Figure 3 Model of *Plasmodium falciparum* merozoite invading an erythrocyte at apical region (20)

1.2 Myosin

Myosin constitutes a large superfamily of proteins that share a common domain which has been shown to interact with actin, hydrolyze ATP and produce movement in all cases examined to date (23). Myosins are typically constructed of three functional subdomains: (1) the motor domain which interacts with actin and binds ATP, (2) the neck domain which binds light chain or calmodulin and (3) the tail domain which serves to anchor and position the motor domain so that it can interact with actin. The motor domains are relatively conserved with the exception of several surface loops and the amino-terminus. Light chains and calmodulin bind to a helical sequence termed the IQ motif found in the neck which has a concensus sequence of IQXXXRGXXXR. The number of IQ motifs present in the necks of different myosins can vary between zero and six. The tail domains are the most diverse domains and vary widely in length and in sequence. In addition, the tails of many myosins contain coiled-coil forming sequences which allow the molecules to dimerize and produce two-headed molecules.

Myosins play fundamental roles in eukaryotic motility. They are implicated in a number of important cell functions including cytokinesis and organelle transport and trafficking. Myosins are also important in cell polarization and signal transduction The functions of each class of myosin have been shown to be distinct. Class I is implicated in endocytic and exocytic membranes traffic, whereas class II, or conventional myosin, is known to be a component of the contractile ring in dividing cells and sarcomere in muscle cells. Myosin III is localized to the photoreceptor cells in the retina and functions in signal transduction. Myosin V and XI have been shown to be organelle motors in animals and plants, respectively. Myosin VI has been shown to move toward the minus end of actin filaments; therefore, it is a reverse motor, and one that is important for development in many multicellular organisms. The 12 other classes of myosin all possess specific functional properties, although most have not been characterized biochemically (24).

1.2.1 Myosin superfamily

The distinct myosin are grouped based on phylogenetic analysis of their head domain. Analysis of the whole molecule or of the tail domains alone generally gives the same relationship (25). The known myosin now can be classified into 18 classes (see Figure 4).

1.2.2 Myosin structure

Myosin is a hexamer with a total molecular weight of 520 kDa. It is composed of one pair of myosin heavy chain (MHC, ~200 kDa) and two pairs of each of the chemically distinct light chains. One class of light chain is termed myosin essential light chain (ELC) or myosin alkali light chain. The ELC is, in fact, composed of two proteins of ~25 kDa and ~16 kDa, which are termed myosin light cahin-1 (MLC-1) and myosin light chain-3 (MLC-3), respectively. The other class of light chain is ~20 kDa and is termed myosin regulatory light chain (RLC) or myosin light chain-2 (MLC-2) as shown in Figure 5 (26).

1.2.2.1 Myosin heavy chain (MHC)

Myosin heavy chain (MHC) is a highly asymmetric molecule. The N-terminal half of MHC forms a globular head, whereas the C-terminal half forms a long alpha-helical tail. The tail (C-terminal) region is periodically interspersed with hydrophobic residues to give a ‘coiled coil’ type rod. The amino acids in the C-terminal are non-helical which aids in stabilizing the myosin filament backbone. Furthermore, the backbone contains inter-myosin ionic bonds to assist in stabilization. The tails are connected to the heads at the neck, which is the location of the hinge area. Proteolytic enzymes divided myosin heavy chain (MHC) into two main fragments: the N-terminal HMM (heavy meromyosin, ~150 kDa) and C-terminal LMM (light meromyosin,~70 kDa). The HMM fragment can be further subdivided into a S1 subfragnent (~95 kDa), corresponding to the myosin head, and a S2 subfragment (~55 kDa), corresponding to the N-terminal portion of the tail.

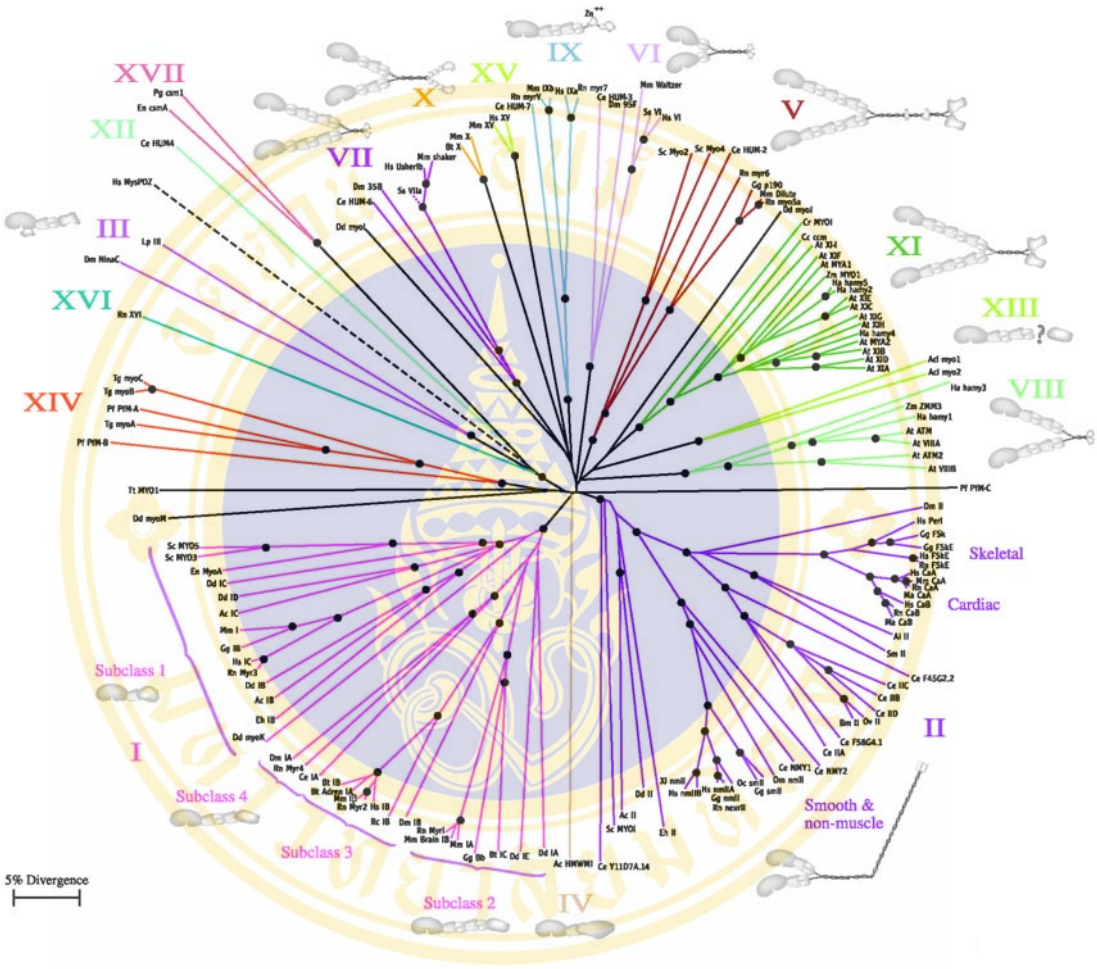

Figure 4 Phylogenic tree obtained from neighbor joining analysis of the myosin motor domain protein sequences

(http://www.mrc-lmb.cam.ac.uk/myosin/trees/trees.html#ref2).

The LMM has been shown to contain a specific region necessary for filament formation (the assembly subdomain), as well as sites of phosphorylation shown to be important for regulating filament assembly in nonmuscle cells. The myosin rods aggregate in an anti-parallel fashion, giving rise to a bipolar structure with a central bare region. The globular head (S1) of MHC contains the actin binding site and the ATP hydrolysis site. The S1 subfragment has been shown to be sufficient to support movement of actin filaments on a nitrocellulose-coated surface in vitro, demonstrating that the minimum requirements for producing motility are contained within the myosin head.

1.2.2.2 Myosin essential light chain

Myosin essential light chain (ELC) is also a number of troponin C superfamily, and contains one functional Ca^{2+}-binding site in region III. The name “the essential light chain” derives from the finding that alkaline conditions used for the initial isolation of ELC resulted in loss of the myosin ATPase activity. However, ELC was later shown not to be essential for myosin function, since enzymatically active myosin devoid of ELC was obtained with a different isolation procedure. It has also been called “the alkali light chain” based on conditions initially used for its extraction.

Although the role of ELC has not been well characterized in most muscle systems, varying isoforms of ELC have been correlated with different maximal velocities of shortening and ATPase activates in skeletal and smooth muscles.

1.2.2.3 Myosin regulatory light chain (MLC-2)

The myosin regulatory light chain (RLC; hereafter called myosin light chain 2, MLC-2) was found to be involved in regulation in various muscle types and nonmuscle cells. MLC-2 is a Ca^{2+}-binding protein, which shares a common ancestor with myosin essential light chain (ELC) troponin C parvalbumin, and calmodulin. It has been proposed that the prototype protein contained four

Ca^{2+}-binding sites (27). The four Ca^{2+}-binding sites are designated I through IV. Some genes that are related to the ancestral prototype encode proteins that have lost their Ca^{2+}-binding ability at some or all of these sites. However, the sites in these proteins have maintained a similar primary and tertiary structure. Direct Ca^{2+}-binding to MLC-2 occurs *in vivo*, and whether this binding is involved in regulation of contraction in most muscle types is not known.

1.2.3 Regulation of actin-myosin II contraction in non muscle cell and smooth muscle cell.

Contraction is regulated primarily by phosphorylation of light chain (Figure 6). Phosphorylation of MLC in these cells has at least two effects: it promotes the assembly of myosin into filaments and it increases myosin catalytic activity, enabling contraction to proceed. The enzyme that catalyzes this phosphorylation, called myosin light chain kinase (MLCK), is itself regulated by association with the Ca^{2+}-binding protein calmodulin. Increases in cytosolic Ca^{2+} promote the binding of calmodulin to the kinase, resulting in phosphorylation of the myosin light chain (MLC). Increases in cytosolic Ca^{2+} are thus responsible, albeit indirectly, for activating myosin in smooth muscle and nonmuscle cells.

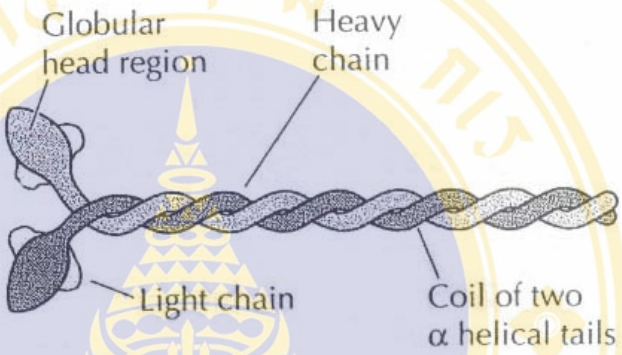

Figure 5 The myosin II molecule. This consists of two heavy chains and two pairs of light chains (called the essential and regulatory light chains). The heavy chains have globular head regions and long alpha-helical tails, which coil around each other to form dimers (26).

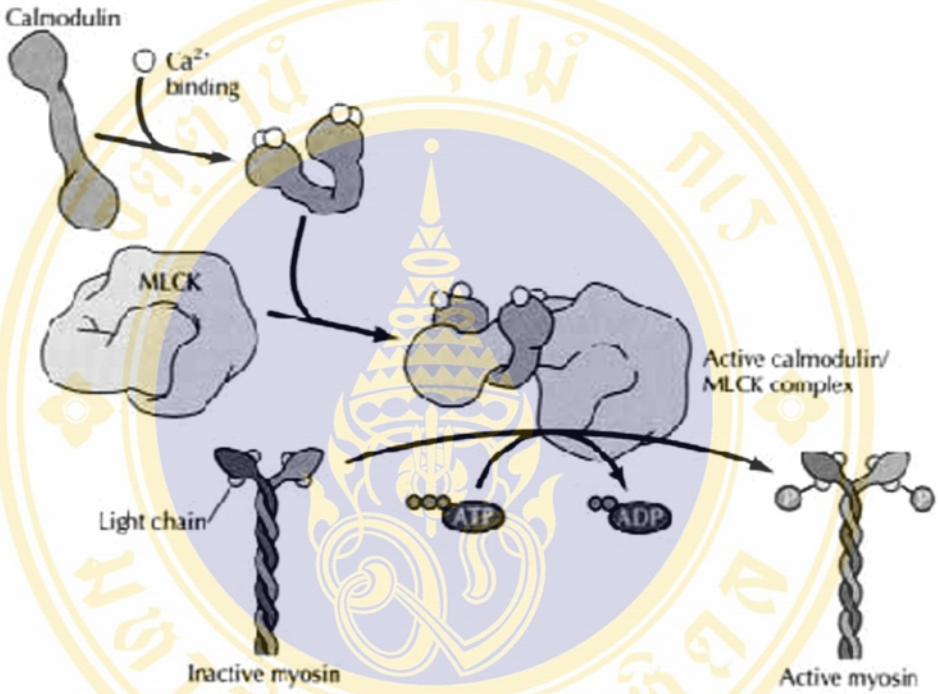

Figure 6 Regulation of myosin by phosphorylation. Ca^{2+} binds to calmodulin, which in turn binds to myosin light chain kinase (MLCK). The active calmodulin-MLCK complex then phosphorylates the myosin II regulatory light chain, converting myosin from an inactive to an active state (26).

1.3 Erythrocyte myosin

Normal human erythrocyte is a symmetrical biconcave disc~7-8 μm in diameter. The mechanical properties of the human erythrocyte are determined by a cytoskeletal network underlying the membrane that is thought to consist of many short actin filaments (~12-20 monomers long) cross-linked by long, flexible spectrin molecules in association with a 80 kDa helper protein, band 4.1. The cytoskeletal network is multiply attached to the cytoplasmic surface of the membrane via the interactions of spectrin and band 4.1 with ankyrin and glycophorin, respectively. Ankyrin is a 210 kDa protein, which is itself tightly associated with band 3, the anion channel and major integral membrane protein, and glycophorin is the major transmembrane sialoglycoprotein in the erythrocyte membrane.

Human erythrocyte myosin consists of a 200 kDa heavy chain and light chains of 26- and 19.5 kDa. At low ionic strength, the myosin forms short bipolar filaments like those of platelet myosin. Like most myosins, it has a high ATPase activity in the presence of Ca^{2+} or EDTA, but is inhibited by Mg^{2+}. Turkey gizzard myosin light chain kinase transfers one phosphate from ATP to the 19.5 kDa light chain (which could be homologous to the 20 kDa regulatory light chain of other cytoplasmic myosins), and this stimulates the actin-activated ATPase (28). It means that the ATPase activity of erythrocyte myosin is stimulated by Ca^{2+} or EDTA but is inhibited by Mg^{2+} and is refractory to actin stimulation unless the 19.5 kDa light chain is first phosphorylated by myosin light chain kinase. The erythrocyte myosin is 150 nm long and is present in about 6,000 copies per cell which is 100 times less than in platelets (29). Similar to other non-muscle myosins, the erythrocyte myosin is capable of self-association into bipolar filaments 200-300 nm long at physiologic salt concentration. In erythrocytes, the estimated concentration of 50 μg/ml is sufficiently high for myosin to form bipolar filaments; this has led to the suggestion that erythrocyte shape changes might be mediated by an ATP-dependent actin-myosin contractile mechanism. In erythrocyte, myosin is distributed in a punctate fashion and seems to be loosely bound to membranes during fractionation. This further led to the suggestion that myosin might act at specialized foci such as spectrin-actin-protein4.1 complexes, where force might be transmitted to the membrane skeleton, which plays a role in

shape change, and thus to the overlying membrane (30). Protein 4.1 partially inhibit the actin –activated Mg^{2+}-ATPase activity of rabbit skeletal muscle myosin showing that protein 4.1 binds to myosin and can regulate its actin-activated Mg^{2+}-ATPase. In addition, the presence in erythrocytes of calmodulin (31), caldesmon (32), tropomyosin (30), and myosin light chain kinase (33). These results taken together raise the possibility of the presence of a Ca^{2+}-dependent actomyosin II ATPase activity in the erythrocyte (34). The role of spectrin-actin-protein 4.1 complex as the locus of myosin action in erythrocyte is as shown in Figure 7 (35).

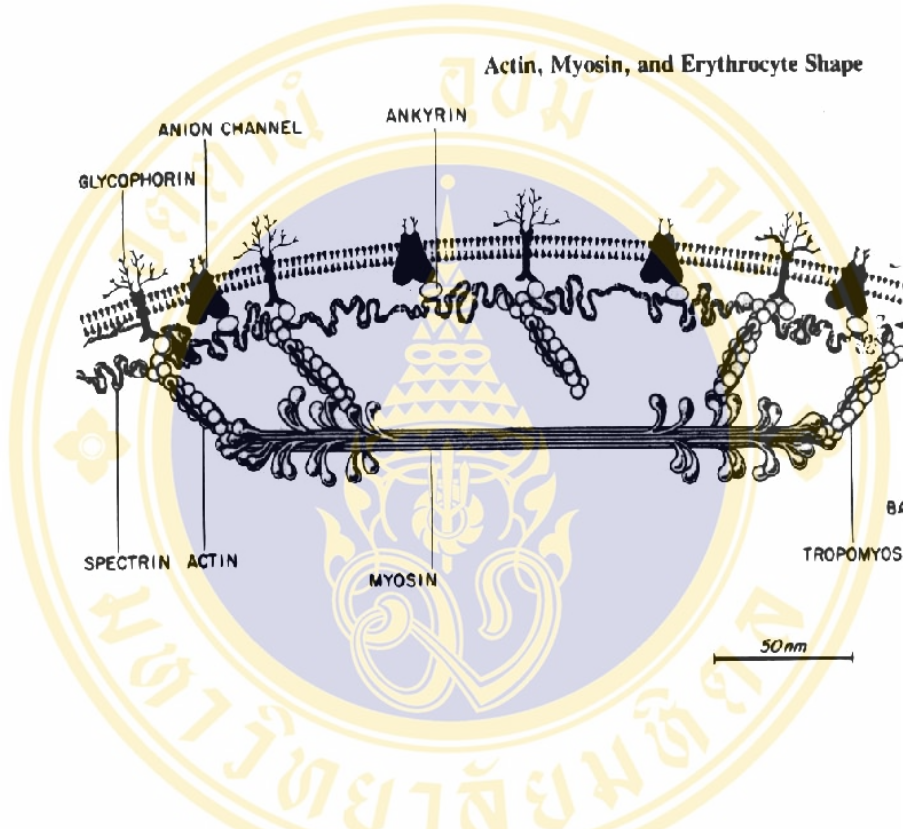

Figure 7 Erythrocyte myosin linkage to others proteins (35)

1.4 *Plasmodium falciparum* myosin

Phylogenetic analysis of myosins places Apicomplexan myosin as a novel class XIV. Mechanisms for regulation of this kind of myosin still unknown. Direct regulation of the activity of the myosin motor domain can be achieved by a variety of mechanisms. These include Ca^{2+} binding to the regulatory light chain (RLC), the phosphorylation of the RLC or the phosphorylation of a site in the motor domain of the heavy chain (36-39). Some of the apicomplexan myosins do not contain IQ motif that bind calmodulin and calmodulin related proteins. Some of them do not follow the TEDS rule, i.e., the presence of negatively charge (E and D) or phosphorylatable residue (T and S). In lower eukaryotes, as in *Dictyostelium* myosin I, phosphorylation of this residueby myosin I heavy chain kinase (MIHCK) is crucial for activation of their ATPase activities by actin (37). Both the absences of an IQ motif and the nonadherence to the TEDS rule suggest that these motors may be regulated in a novel fashion (40). The apicomplexa may have evolved and subtly diversified their own unique set of myosins to accomplish all of the cellular function such as cell motility, intracellular transport, endocytosis, and signal transduction that are accomplished by a different and greater diversity of myosins in other cell types (41).

There are four types of *P. falciparum* myosin: Pfmyo-A, Pfmyo-B, Pfmyo-C and Pfmyo-D. Pfmyo-A and Pfmyo-B are both ~93 kDa. Pfmyo-C is a large ~240 kDa myosin (41). Pfmyo-A is expressed in invasive stage, both sporozoite and merozoite. The expression and function of others *P. falciparum* myosins have not been reported. *Plasmodium* myo-A was also identified in *P. berghei* and *P. yoleii* sporozoites (42). Pfmyo-C and Pfmyo-D both contain negatively charge residue (E) in TEDS motif. Additional domains recognized are described in Table I with those of most significance occurring in tail regions (e.g., for Pfmyo-C: WD40 repeats and the RGD adhesion site) (43).

TABLE I. Features of Apicomplexan Myosins and Positions of Domains

Myosin	ATP binding sites (myosin heavy chain)	TEDS rule[a]	IQ domain sequences[b]	Actin binding sites	Additional domains[c]
PbmyoA AF255909	108 GESGAGKT	334 N	None recognised	578 PHFIRCIKPNE	Common motifs only
PbmyoA AF286048	191 GESGAGKT	417 N	None recognised	661 PHFIRCIKPNE	Common motifs only
PbmyoA	191 GESGAGKT	417 N	None recognised	661 PHFIRCIKPNE	Common motifs only
PfmyoA	191 GESGAGKT	417 T	None recognised	661 PHFIRCIKPNE	606 "RGD" putative cell adhesion site[d]
Tgmyo-A	193 GESGAGKT	419 Q	None recognised	663 PHFIRCIKPND	791 putative amidation site[e]
BbmyoA	169 GESGAGKT	323 N	None recognised	570 SHFIRCVKPNE	Common motifs only
Tgmyo-D	189 GESGAGKT	415 N	None recognised	660 SHFIRCIKPND	483 Glycosyl hydrolase family 5 signature (cellulase)[f]
Tgmyo-E	200 GESGAGKT	429 Q	None recognised	673 SHFIRCLKPNE	219 putative amidation site[e]
Tgmyo-B/C	129 GESGAGKT	354 Q	720 LGPMWRKVLLRK	601 AHFIRCLKPNE	Common motifs only
BbmyoB	190 GESGAGKT	413 D	689 IQTIHRGFAYRT	654 SHFIRCIKTNQ	Myosin- N domain[g]
Pfmyo-B	178 GESGSGKT	401 Q	None recognised	643 IYFIKCIKPNE	Common motifs only
	353 GIEKGGKS				
Pfmyo-C	90 GESGAGKT	387 E	848 IQKNYKTYTQKKL	637 PHFIRCIKPNA	1844 WD40 repeats[h]
	1324 GPRNVGKT		872 IQRWFRNRLNIIRK		308 Cysteine protease active site[i]
			920 IQSHIRRYLMVRF		352 Leucine zipper - coiled coil[j]
			945 IQATWKAYKEHLF		1604 "RGD" putative cell adhesion site[d]
			968 IQLKWKSILARK		
Pfmyo-D	207 GHSGSGKT	588 E	1128 SQKYNRDEGDHN	1020 MYYIRCILPND	Long stretches of Asn residues both within the head and tail domains.

[a]TEDS rule: Tendency for myosins to contain a phophorylatable residue (T or S) or a negatively charged residue (E or D) at a site 16 positions upstream from the conserved DALAK sequence [Bement and Mooseker, 1995].

[b]Putative IQ motif for light chain or calmodulin binding, Consensus IQXXXRGXXXRK, common to neck region of myosin molecules that can contain zero to 6 of these motifs [Cheney and Mooseker, 1992]. Divergent IQ sequences in *T. gondii* B/C myosins were discussed by Heintzelman and Schwartzman [1997] and Hettmann et al. [2000]. "None" indicates that no recognisable IQ motif was identified.

[c]Motifs, searched using motifs program, common to all myosins in the table (and frequently occurring in proteins) are: N-glycosylation sites; Kinase phosphorylation sites, glycosaminoglycan attachment site, and N-myristoylation sites. Those listed in this column are additional to this list and not common to all other myosins in the table. PFAM was also used to search for domains and results were consistent with results obtained using Motifs.

[d]Arg-Gly-Asp has been called the RGD tripeptide shown to play a role in cell adhesion in a number of proteins, e.g., collagens, fibrinogen [D'Souza et al., 1991], within the head domain for Pfmyo-A and the tail of Pfmyo-C.

[e]C-terminal amidation is the site of cleavage for precursors of hormones and other active peptides; these have not been shown to occur in unicellular organisms or plants [Bradbury and Smyth, 1987]. One site is within start of the tail region of Tgmyo-A and one is identified within the head domain downstream from the ATP binding site of Tgmyo-E.

[f]Glycosyl hydrolase family 5 signature common to fungal or bacterial cellulolytic enzymes [Henerissat, 1991] within the head domain.

[g]Bbmyo-B contains an "Myosin N-terminal SH3-like domain", which was not recognised in any other Apicomplexan myosin described here. This domain has an SH3-like fold. It is found at the N-terminus of many but not all myosins. The function of the domain is unknown (see http://www.sanger.ac.uk/Pfam/).

[h]Trp-Asp (WD40) repeats are linked to membrane anchoring and receptor recognition [Gilman, 1987]; this is within the tail domain.

[i]Active site for eukaryotic cysteine proteases [Dufour, 1988]; this sequence is within the head domain region.

[j]Leucine zipper pattern is a structure proposed to explain the activity of eukaryotic regulatory proteins, particularly nuclear DNA binding proteins [Landschulz et al., 1988]. Coiled coils recognised in myosin tails apparently allow the molecules to dimerize and produce two-headed molecules [Sellers, 2000]; this coiled coil is within the head domain of Pfmyo-C.

1.5 ML-7

ML-7 (1-5-iodonapthalene-1-sulfonyl)-1H-hexahydro-1,4-diazepine hydrochloride) is a synthetic MLCK inhibitor which was found to be a potent and selective inhibitor of MLCK. This compound inhibits both Ca^{2+}-calmodulin dependent and independent smooth muscle myosin light chain kinase to a similar extent, and its inhibition is of the competitive type with respect to ATP-binding site on the kinase molecule (44). The structure is shown in Figure 8. Ki values for myosin light chain kinase (MLCK) and other kinases are shown in Table 2.

1.6 BDM

BDM (2,3-butanedione monoxime) is myosin ATPase inhibitor. It has been widely used as a non-muscle myosin inhibitor. BDM was introduced to the cell biology community as a millimolar inhibitor of multiple non-muscle myosins with greatest potency in inhibiting non-muscle myosin II. BDM also inhibits the ATPase activity of purified myosin V and of a *Drosophila* protein fraction that mostly contains cytoplasmic myosin and myosin VI as well as other unidentified actin-binding proteins. BDM does not inhibit kinesin ATPase activity or the *in vitro* polymerization of rabbit muscle actin. It rapidly and reversibly inhibits cell spreading of PtK2 cell line in about 16 min. (45). BDM appears to interact specifically to myosin.ADP.Pi complex and decrease the rate of Pi release (46). The structure is shown in Figure 9.

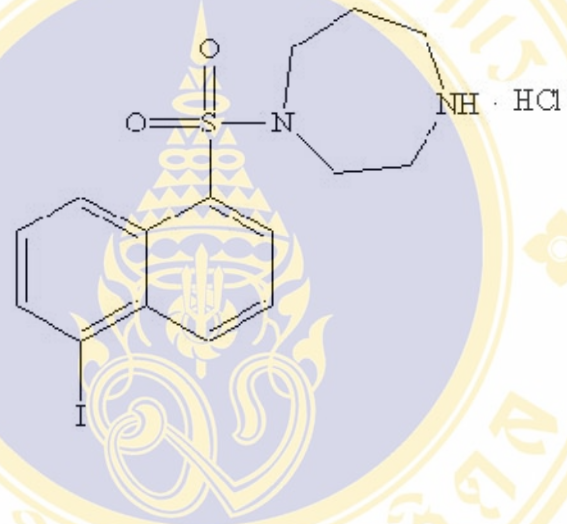

Figure 8 Structure of MLCK inhibitor (ML-7)

Table 2 Ki values for myosin light chain kinase (MLCK) and other kinases

Protein kinase	Ki (μM)
MLCK	0.3
PKA	21
PKC	42

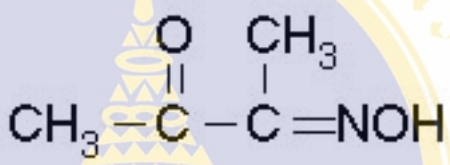

Figure 9 Structure of myosin ATPase inhibitor (BDM)
(http://sigmaaldrich.com)

CHAPTER 2
OBJECTIVES

The goal of this study was to investigate possible involvement of the myosin-based contractile system in *Plasmodium falciparum* development within the human erythrocyte, and in invasion of the erythrocyte. The specific aspects are

1. To assess the effects of myosin inhibitors (BDM and ML-7) on the development of *Plasmodium falciparum* inside the erythrocytes from ring to trophozoite, and from trophozoite to schizont, respectively.
2. To assess the effects of myosin inhibitors (BDM and ML-7) on the efficiency of *Plasmodium falciparum* development from schizont to ring stage (erythrocyte invasion).
3. To assess the combination effects of myosin inhibitors (BDM and ML-7) on *Plasmodium falciparum* growth within the erythrocyte.

CHAPTER 3
MATERIALS AND METHODS

3.1 Materials

3.1.1 Malaria parasite

K1 strain of *Plasmodium falciparum* (chloroquine and pyrimethamine resistant), originally isolated from a malarial patient in Kanchanaburi Province, Thailand (47), was maintained in continuous culture *in vitro* using candle-jar culture technique described by Trager and Jensen (48, 49).

3.1.2 Materials for cultivation of *P. falciparum*

1. RPMI-1640 powder was product of GIBCO., NY, USA.
2. Human erythrocytes (O, Rh+) from local blood donors were kept at 4 ^{o}C in blood bags containing anticoagulant, acid-citrate-dextrose (ACD).
3. Human serum (group A,B,AB or O) was stored at –20 ^{o}C.
4. Gentamicin (80mg/2ml) was purchased from The Government Pharmaceutical Organization., Thailand.
5. 60 x 15 mm tissue culture plastic petri dish was purchased from CORNING., NY, USA.
6. 100 x 20 mm tissue culture plastic petri dish was purchased from CORNING., NY, USA.
7. 0.45 μm Millipore filter from Whatman., Maidstone England, England.

3.1.3 Materials for drug susceptibility testing

1. 1-(5-iodonaphthalene-1-sulfonyl)-1H-hexahydro-1,4-diazepine (ML-7), myosin light chain kinase inhibitor, was purchased from Sigma Chemical Co., MO, USA.
2. 2,3-butanedione monoxime (BDM), myosin ATPase inhibitor, was purchased from Sigma Chemical Co., MO, USA.
3. [^{3}H]-hypoxanthine (specific activity of 21 Ci/mmol) was purchased from Amersham, UK.
4. 96-wells microculture plastic plates were purchased from NUNC., Roskilde, Denmark.
5. Glass filter paper grade 943 AH was from Whatman., Maidstone England, England.
6. Minicell harvester was from NUNC., Roskilde, Denmark.
7. Liquid scintillation counter LS1801 was from Beckman, Irvine, USA.
8. IEC International centrifugation, model PR-2.

3.1.4 Miscellaneous chemicals

Name of chemicals	**MW**	**Company**
Dimethyl sulfoxide (DMSO)$(CH_3)_2SO$	-	Merck
Ethanol, absolute (CH_2OH)	46.07	Merck
Glycerol ($C_3H_8O_3$)	92.09	Carlo Erba
2,4 diphenyloxazole (PPO)	221.3	Sigma
(1,4-bis[2-(5-phenyloxazole)]benzene)(POPOP)	364.4	Sigma
Di-potassium hydrogenphosphate (K_2HPO_4)	174.18	Merck
Di-sodium hydrogenphosphate(Na_2HPO_4)	141.96	Merck
D-sorbitol ($C_6H_{14}O_6$)	182.18	Fluka
Toluene ($C_6H_5CH_3$)		Shell Chemicals

3.2 Methods

3.2.1 *In vitro* cultivation of *Plasmodium falciparum*

3.2.1.1 Preparation of materials for cultivation

Parasites were maintained in continuous culture by a method based on that of Jensen and Trager (48, 49).

3.2.1.1.1 RPMI-1640 stock medium

Ten point four gram of RPMI medium was initially dissolved in 800 ml of distilled water then 5.94 g of HEPES were mixed in to give a final concentration of 25 mM HEPES. Total volume was adjusted to 960 ml with distilled water to give pH 6.75. An antibiotic, gentamicin, was added to the medium solution at a final concentration of 40 μg/ml to inhibit bacterial contamination. Finally, the medium was filtered through a 0.45 μm Millipore filter. The solution was aseptically dispensed as 100 aliquots into sterilized bottle and stored at 4 ^{o}C for use within one month.

Incomplete medium

The incomplete medium was used for washing erythrocytes and preparing working drug solutions.

Four point two milliliter of 5% (w/v) $NaHCO_3$ solution was added to 100 ml of stock RPMI-1640 medium to give a final concentration of 0.2 % (w/v) $NaHCO_3$. As a result, solution turned from yellow to orange, indicating a shift in pH 6.75 to 7.4, and was kept at a 4 ^{o}C. The medium was used before the color turned to red which indicates the shift to alkaline pH resulting from loss of CO_2.

Complete medium

For cultivation, complete medium was prepared by adding 5% $NaHCO_3$ solution and 11.5 ml of O type, Rh^+ human serum to give a final concentration of 0.2% (w/v) $NaHCO_3$, and 10% serum, respectively. The solution was kept at 4 ^oC for use within one week.

3.2.1.1.2 Sodium bicarbonate, 5%(w/v)

Five gram of $NaHCO_3$ was dissolved in 100 ml of distilled water. After sterilization by filtration through a 0.45 μM Millipore filter, 10 ml aliquots were made and kept at 4 ^oC for use within one month.

3.2.1.1.3 D-sorbitol, 5% (w/v)

Five percent of D-sorbitol was prepared in the same manner as that of 5 % (w/v) $NaHCO_3$.

3.2.1.1.4 Serum

Fresh human serum was obtained from whole blood collected without anticoagulant. The blood was allowed to clot for 3-4 h at room temperature, and the clotted blood was stored overnight at 4 ^oC to allow clot retraction. After centrifugation at 2,000 rpm (IEC model) at 4 ^oC for 10 min, serum was obtained and aliquoted in 11.5 ml for storing at –20 ^oC and for use within three months.

3.2.1.1.5 Uninfected erythrocytes

Human blood O type (Rh+) was collected in plastic bags containing ACD (acid citrate dextrose as anti-coagulant). Fifty-milliliter aliquots were transferred into 100 ml screw-capped bottles and stored a 4 ^oC. Before use, a desired volume, usually 10 ml. was centrifuged in a 50 ml tube at 2,000 rpm at 4 ^oC

for 10 min. After removal of plasma and buffy coat, packed cells were washed twice with incomplete medium. The cells were then resuspended in the complete medium to obtain a 50% (v/v) cell suspension, kept at 4 ^{o}C and used within one week.

3.2.1.2 Cultivation procedure

P. falciparum-infected erythrocytes were prepared from either continuous culture or frozen culture. In case of continuous culture, the culture was centrifuged in a 50 ml tube at 2,000 rpm 4 ^{o}C for 10 min before the supernatant was discarded, and the cells were resuspended in an equal volume of complete medium. Thin films were examined to determine the degree of parasitemia by counting the number of viable parasites per 1,000 erythrocytes.

To obtain an appropriate parasitemia level (0.3-0.5%parasitemia), washed erythrocytes (50%(v/v)) were added to the culture. 0.5 ml aliquots of this cell suspension were then dispensed into 60 x 15 mm plastic culture petri dishes and 10 ml of complete medium were added to give a final 3% cell suspension. The petri dish was then placed in a dessicator containing a white candle. The stopcock-cover was tightly sealed with silicone grease. The candle was lit while the stopcock was still open. When the candle flame went out, the stopcock was closed immediately, producing an atmosphere with relatively low CO_2 and high O_2 content (17% O_2, 3% CO_2, 80% N_2 (2)). The dessicator was then placed in an incubator at 37 ^{o}C.

Fresh erythrocytes were routinely added every three or four days to the culture plates providing the parasitemia did not exceed 6-8%. The medium was changed manually once a day by gently tipping the dish and withdrawing the old medium with sterilized pasteur pipets. Disturbance of settled red cells was kept to minimum and as much fluid as possible was removed without taking out the cells. Ten milliliter of fresh medium were added back to the culture dish, mixed gently and placed in the candle jar. It is important that this procedure is strictly followed so as to prevent excess pH shift and high glucose consumption rate, which would lead to parasite death.

3.2.1.3 Parasitemia determination

The level of parasitemia was estimated by counting the number of viable parasites per 1,000 erythrocytes on a thin blood film after Giemsa's staining. Thin smear was made by first removing the medium from the settled red cells and then spreading a small amount of cells on a slide, which was then air dried, fixed with methanol, and then stained with 5% Giemsa's stain at pH 7.2 for 10 min (Appendix).

3.2.1.4 Cryopreservation of malarial parasites

3.2.1.4.1 Freezing

The culture material with more than 5% parasitemia at mostly ring stage was centrifuged at 2,000 rpm at 4 ^{o}C for 10 min. After the supernatant was discarded, cells were resuspended in an equal volume of freezing solution (28% glycerol, 3% sorbitol and 0.65 % NaCl) and mixed well. The aliquots containing 0.5 ml of cell suspension were quickly frozen by immersing the vials into liquid nitrogen.

3.2.1.4.2 Recultivation of frozen malaria

The frozen culture vials were retrieved from liquid nitrogen. The screw caps of vials were slightly loosened and set upright in water, then the thawed suspension was centrifuged at 2,000 rpm for 10 min. The supernatant was discarded and the cells were resuspended in an equal volume of sterilized hypertonic saline solution (3.5% NaCl). The suspension was gently mixed before centrifugation at 2,000 rpm for 10 min, and the supernatant was removed again. After washing twice with an equal volume of incomplete medium, the cells were finally resuspended in an equal volume of complete medium to give 50% cell suspension. Then the uninfected erythrocytes were added to obtain the desired parasitemia level.

3.2.1.5 Synchronization of *P. falciparum*

3.2.1.5.1 Synchronization of ring-stage parasite

Ring stage of *P. falciparum* was synchronized as described by Lambros and Vanderberg (50). *In vitro* culture of *P. falciparum*, in which all stages of asexual parasites were present, was centrifuged at 2,000 rpm (IEC model) at 4 ^{o}C for 10 min and the supernatant was removed. The packed cells were thoroughly resuspended with 5 volume of sterile 5%(w/v) D-sorbitol aqueous solution and incubated at room temperature for 10 min. During this treatment, a selective destruction of late stage malaria infected erythrocytes (late trophozoite and schizont) occurred, leaving only ring stage infected cells. These were harvested by centrifugation at 2,000 rpm for 10 min, washed twice with incomplete medium, and diluted with washed uninfected erythrocytes to an appropriate percent parasitemia.

After 48 h in culture, ring stage of the next cycle appeared. These were further used for testing the inhibitory effect of the myosin inhibitors against *P. falciparum* growth and development from ring to trophozoite stage.

3.2.1.5.2 Synchronization of trophozoite-stage parasite

Synchronized ring-stage parasites were cultured for 22-24 h, to allow development to trophozoite stage. The trophozoites obtained were used for testing the inhibitory effect of the inhibitor against *P. falciparum* development from trophozoite to schizont stage.

3.2.1.5.3 Synchronization of schizont-stage parasite

Percoll, a colloidal silica medium coated with polyvinylpyrrolidone, was used for density gradient centrifugation to separate schizonts from other stages and uninfected erythrocytes as described by Kusmith (51).

Percoll was diluted by sterile 1XPBS pH 7.4 to obtain 40, 50, 60 and 75 %percoll. The percolls were layered with decreasing density from bottom to top of centrifuge tube.

After the culture of synchronized ring stage were grown for 36 h, they (> 10-20 %parasitemia) were collected into a centrifuge tube and centrifuged at 2,000 rpm for 10 min in a refrigerated centrifuge (IEC). The supernatant was discarded and the packed cell was resuspended as 50% cell suspension with complete medium. The cell suspension was overlaid onto 40% Percoll layer with minimum disturbance of the Percoll surface. The suspension was then centrifuged at 2,000 rpm for 20 min at 4 ^{o}C. The upper layer (brown interphase) which contains schizonts was washed twice with incomplete medium before being used for testing the inhibitory effect.

3.2.2 The *in vitro* susceptibility test

The susceptibility of the parasites to various inhibitors were determined by [^{3}H]-hypoxanthine incorporation method modified from that described by Desjardins *et al* (52).

3.2.2.1 Inhibitor preparation

Inhibitors were initially dissolved in suitable solvent (e.g., incomplete medium (ICM), distilled water (DW), ethanol (EthOH)) to get a stock concentration. For ML-7, it was diluted with 1:1 of ethanol:distilled water to get a stock concentration of 20 mM and kept under –20^{o}C. BDM was freshly diluted with incomplete medium to appropriate concentration just before use. The effect of solvents were also tested and designated as “controls”.

3.2.2.2 Preparation of parasitizied erythrocytes

The synchronized ring stage cultures were placed in 15 ml centrifuge tubes and centrifuged at 2,000 rpm for 10 min. The supernatant was discarded and the packed cells were resuspended in equal volume of complete

medium. Thin films were made to determine the level of parasitemia by counting the number of viable parasites per 1,000 erythrocytes. The parasitemia was adjusted to give a desired final concentration of 1.5% hematocrit with 1% parasitemia by adding 50% (v/v) uninfected erythrocytes.

3.2.2.3 Inhibitor susceptibility test by [^{3}H]-hypoxanthine incorporation method

To each well of a 96-well plate, 25 µl of various inhibitor concentrations were added, followed by 200 µl of the synchronized parasitized erythrocyte suspension to give a final volume of 225 µl/well. The plates were placed in a candle jar, and incubated at 37 ^{o}C for 24 h. 25 µl of 10 µCi/ml ^{3}H-hypoxanthine (specific activity of 21 Ci/mmol) in complete medium were added to yield 1 µCi/well. The plates were then placed in a candle jar and incubated further at 37 ^{o}C for 18-20 h. Control cells are exposed to the solvent in the absence of inhibitor.

After that the cells in each well were harvested onto glass filter paper (Whatman grade 943 AH) by using a minicell harvester. The filters were dried in a hot air oven for 1-2 h before each disk was placed in a 1.5 ml. microtube. A 0.5 ml aliquot of liquid scintillation fluid (0.35%(w/v) PPO and 0.05%(w/v) POPOP in toluene) was added into each tube. The microtubes were then placed in plastic vials for measurement of radioactivity (count per minute) by using a liquid scintillation counter (Beckman LS1801. Irvine, USA). The 50% inhibitory concentration (IC_{50}) value, which was defined as the drug concentration required for 50% reduction of the ^{3}H uptake by parasites as compared to control was determined from the dose-response curve. The results shown represented mean ± S.E.M of percentage of ^{3}H-hypoxanthine incorporation relative to control from three independent experiments, each carried out in triplicates.

3.2.3 Determination of the effect of inhibitors on parasite development

The parasitemia was adjusted to give a final concentration of 2% heamatocrit with 3% parasitemia. To each well of 96-well plate, 25 µl of various

inhibitor concentrations were added, followed by 200 µl of the synchronized parasitized erythrocyte suspension to give a final volume of 225 µl/well. Control cells were exposed to the solvent in the absence of inhibitor. The plates were placed in a candle jar, and incubated at 37 ^{o}C.

For studying the effect of inhibitor on development from ring to trophozoite stages, the culture was incubated for 22-24 h. For trophozoite to schizont stages, the culture was incubated for 16-20 h. The parasitemia was determined by counting the number of infected erythrocytes per 5,000 erythrocytes in Giemsa-stained thin blood films. If the inhibitors had an effect on development of the parasite, the affected stages accumulate. The 50% inhibitory concentration (IC_{50}) of each set of experiment was determined and compared to controls. The results shown represented mean ± S.E.M from three independent experiments, each carried out in triplicates.

In addition, effect of inhibitor on schizont nuclear division was also investigated. In routine continuous culture, mature schizont has 5-16 nuclei so in this experiment, the schizont-stage parasites were classified into 2 groups based on the number of nuclei: immature schizont has 2-5 nuclei whereas mature schizont has more than 5 nuclei. The effect of each inhibitor on maturation of schizont was represented by % maturation, which was calculated as shown below:

$$\% \text{ maturation} = \frac{\text{number of erythrocytes containing mature schizont} \times 100}{\text{total number of erythrocytes containing schizont}}$$

The results shown represented mean ± S.D from three independent experiments, each carried out in triplicates

3.2.4 Determination of the effect of inhibitors on parasite development from schizont to ring stage

The synchronized schizont-stage parasitized cells were adjusted to give a final concentration of 2% hematocrit with 5% parasitemia. To each well of 96-well plate, 25 µl of various inhibitor concentrations were added, followed by 200 µl of the synchronized parasitized erythrocyte suspension to give a final volume of

225 µl/well. Control cells are exposed to the solvent in the absence of inhibitor. The plates were placed in a candle jar, and incubated at 37 ^{o}C for 12-18 h. The parasitemia was determined by counting the number of infected erythrocytes per 1,000 erythrocytes in Giemsa-stained thin blood films. The 50% inhibitory concentration (IC_{50}) of each set of experiment was determined and compared to controls. The results shown represented mean ± S.E.M of percentage of number of ring relative to control from three independent experiments, each carried out in triplicate. In addition, effect of the inhibitor on schizont accumulation was also investigated by counting the parasites at different stage per 1,000 erythrocytes in Giemsa-stained thin blood films. The results shown represented mean ± S.D from three independent experiments, each carried out in triplicates.

3.2.5 Method for testing the inhibitor combinations against *P. falciparum* growth

3.2.5.1 Inhibitors preparation

The combinations of inhibitors against *P. falciparum* growth in *in vitro* were tested as described below. From stock solution, the two inhibitors were diluted separately in 1.5 ml microtubes with incomplete medium. A 12.5 µl aliquot of the two inhibitors with different concentrations was mixed together in the wells to obtain a set of inhibitors with combination of various concentrations as shown in following diagram.

BDM \ ML-7	0	1	2	3	4	5	IC_{50}ML-7
0							
2							
3							
4							
5							
IC_{50}BDM							

3.2.5.2 Testing inhibitor combinations against *P. falciparum* growth

After the inhibitors were prepared as describe above, 200 µl of synchronized parasitized erythrocyte suspension (1%parasitemia in 1.5 %hematocrit) were added into each well. The plates were placed in a candle jar and incubated at 37 ^{o}C for 24 h and further experiments were done as in the drug susceptibility test by [^{3}H]-hypoxanthine incorporation method.

The results were expressed as isobolograms, which were constructed from the results of the fractional inhibitory concentration (FIC). FIC was calculated as follows:

$$\text{FIC of ML-7} = \frac{IC_{50} \text{ of ML-7 in combination with BDM}}{IC_{50} \text{ of ML-7 alone}}$$

$$\text{FIC of BDM} = \frac{IC_{50} \text{ of BDM in combination with ML-7}}{IC_{50} \text{ of BDM alone}}$$

The FIC values allowed interpretation on the following criteria: FIC<1, synergistic; FIC=1, additive; FIC>1 antagonistic.

CHAPTER 4
RESULTS

4.1 Effect of myosin II inhibitors on growth of *P. falciparum*

The human erythrocytes contain myosin type II, whereas *P. falciparum* contains myosin type XIV.

The role of myosin II of human erythrocyte during *P. falciparum* infection was examined by incubating *P. falciparum*-infected erythrocytes with the myosin II inhibitors, ML-7 and BDM, by monitoring growth of the parasite from ring to schizont stage using ^{3}H-hypoxanthine incorporation assay. It has been shown that intensive DNA synthesis and nuclear division occur during trophozoite and schizont stages of parasite, rendering the highest ^{3}H-hypoxanthine incorporation during this period of development (53, 54). Increasing concentrations of ML-7 and BDM caused a dose-dependent reduction of ^{3}H-hypoxanthine incorporation into parasite, showing IC_{50} values of 6.3±1.1 μM (Figure 10A) and 6.4±1.1 mM (Figure 10B), respectively.

A.

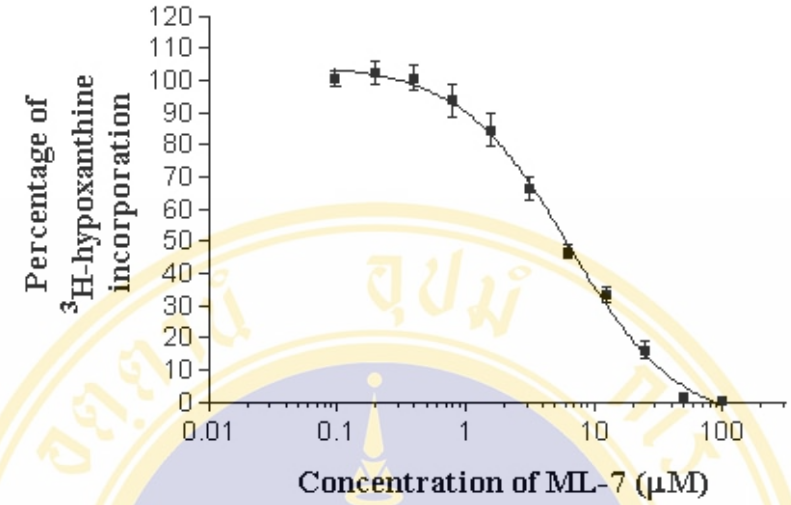

B.

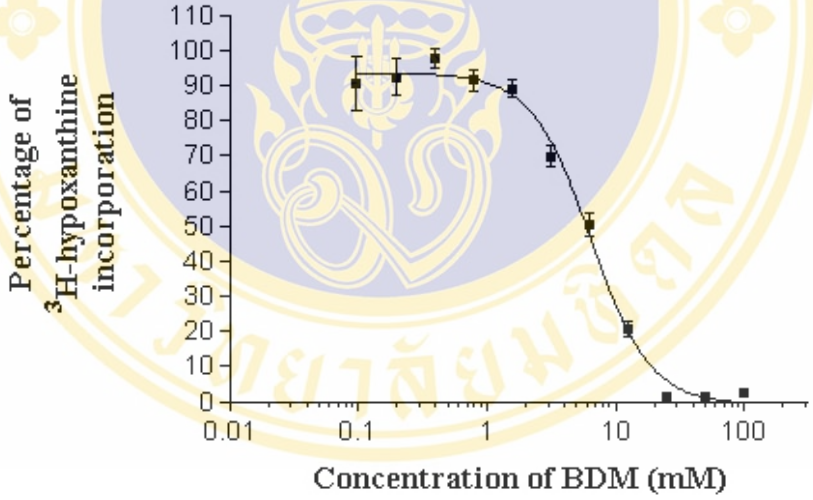

Figure 10 Effect of ML-7 (A) and BDM (B) on ^{3}H-hypoxanthine incorporation during ring to schizont development. The ring-infected erythrocytes were exposed to the inhibitor for 24 h before ^{3}H-hypoxanthine was added. After additional 18-20 h incubation, the parasites were harvested and the radioactivity was measured. The results shown represented mean±S.E.M of percentage of radioactivity (count per minute) relative to control from three independent experiments, each carried out in triplicate. Control cells were exposed to the solvents in the absence of inhibitor.

4.2 Effect of myosin II inhibitors on *P. falciparum* development

The results above showed that both myosin II inhibitors inhibited parasite growth in a dose-dependent manner, suggesting that erythrocyte myosin II plays an important role in supporting parasite development within it. Alternatively, but not exclusively, the myosin II inhibitors may also inhibit parasite myosin XIV function that is essential for parasite development inside the erythrocytes. Due to technical limitation, it is not possible at this stage to inhibit each type of myosin independently, nor to differentiate whether reduction of ^{3}H-hypoxanthine incorporation observed (Figure 10) was due to inhibition of erythrocyte myosin II and/or *P. falciparum* myosin XIV, or both. However, there are further investigation to determine which stage of development, from ring to schizont stage, was sensitive to the inhibitors by examining under a microscope the Giemsa-stained thin blood films of parasite cultures at different stages.

4.2.1 Effect of myosin II inhibitors on development of *P. falciparum* from ring to trophozoite stage

Increasing concentrations of ML-7 and BDM caused a dose-dependent reduction of the number of trophozoites in culture with IC_{50} value of 4.6$\pm$1.3 μM (Figure 11A) and 17.0$\pm$1.4 mM (Figure 11B), respectively.

4.2.2 Effect of myosin II inhibitors on development of *P. falciparum* from trophozoite to schizont stage

Increasing concentrations of ML-7 and BDM caused a dose-dependent reduction of the number of schizonts in culture with IC_{50} value of 43.5$\pm$1.3 μM (Figure 12A) and 10.6$\pm$1.2 mM (Figure 12B), respectively.

A.

B.

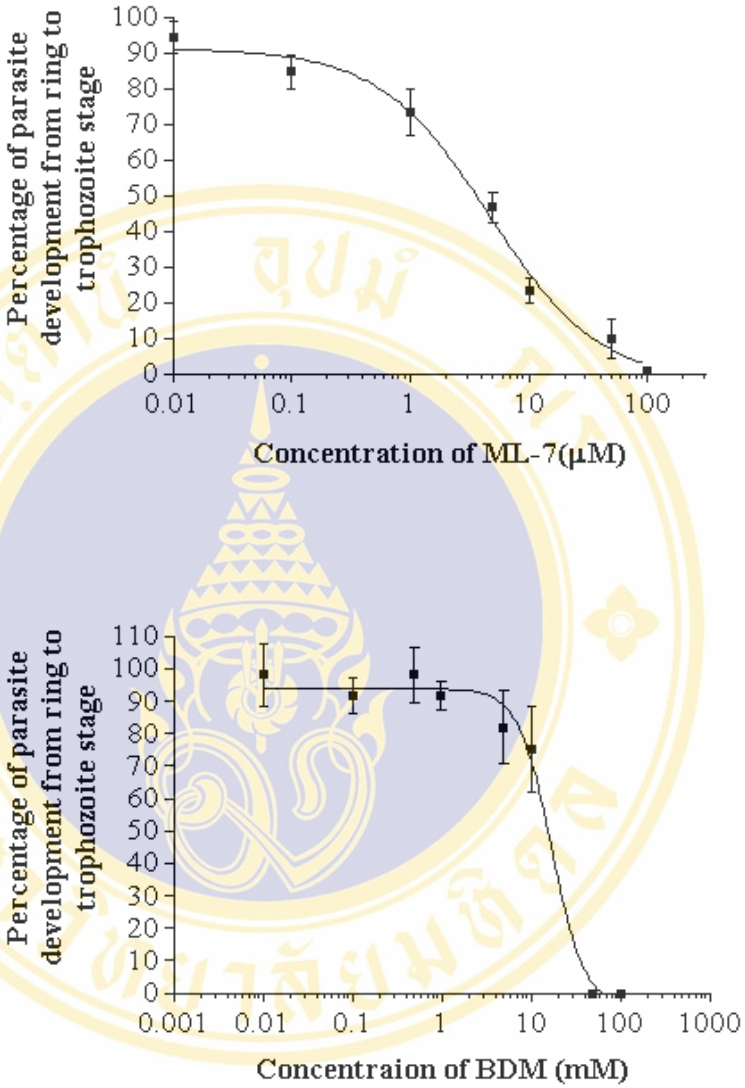

Figure 11 Effect of ML-7 (A) and BDM (B) on *P. falciparum* development from ring to trophozoite stage. Ring-infected erythrocytes at 2% hematocrit and 3% parasitemia were exposed to the inhibitor for 22-24 h before the number of trophozite-infected erythrocyte per 5,000 erythrocytes in Giemsa-stained thin blood films were counted under microscope. The results shown represented mean±S.E.M of percentage of number of trophozoite relative to control from three independent experiments, each carried out in triplicate. Control cells were exposed to the solvents in the absence of inhibitor.

A.

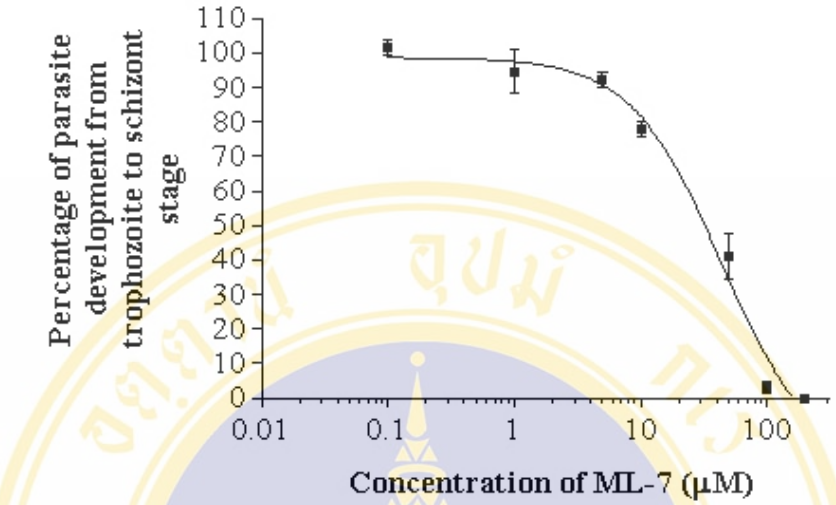

B.

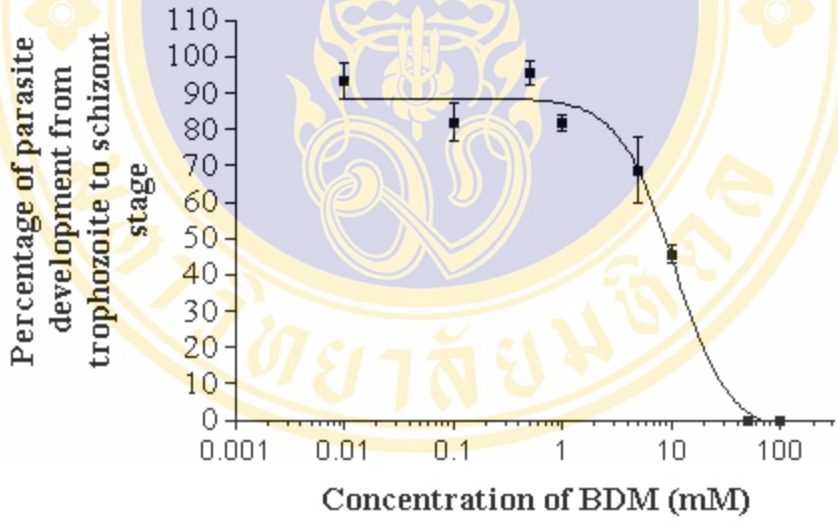

Figure 12 Effect of ML-7 (A) and BDM (B) on *P. falciparum* development from trophozoite to schizont stage. Trophozoite-infected erythrocytes at 2% hematocrit and 3% parasitemia were exposed to the inhibitor for 16-20 h before the number of schizont-infected erythrocyte per 5,000 erythrocytes in Giemsa-stained thin blood films were counted under microscope. The results shown represented mean±S.E.M of percentage of number of schizont relative to control from three independent experiments, each carried out in triplicate. Control cells were exposed to the solvents in the absence of inhibitor.

4.3 Effect of myosin II inhibitors on parasite maturation

As the above results showed that myosin II inhibitors suppressed development of parasite from trophozoite to schizont stage in a dose-dependent manner, There are further investigation to examine if the inhibitors had an effect on the maturation of schizonts by scoring the number of erythrocytes containing mature schizonts (those with more than 5 nuclei) relative to the total number of schizont-infected erythrocytes. Then the percentage of mature schizont was expressed as:

$$\% \text{ maturation} = \frac{\text{number of erythrocytes containing mature schizont} \times 100}{\text{total number of erythrocytes containing schizont}}$$

Figure 13A shows that more than 50 μM of ML-7, was necessary to affect the maturation of schizonts, whereas up to 10 mM of BDM had little, if any, affect on schizont maturation (Figure 13B).

A.

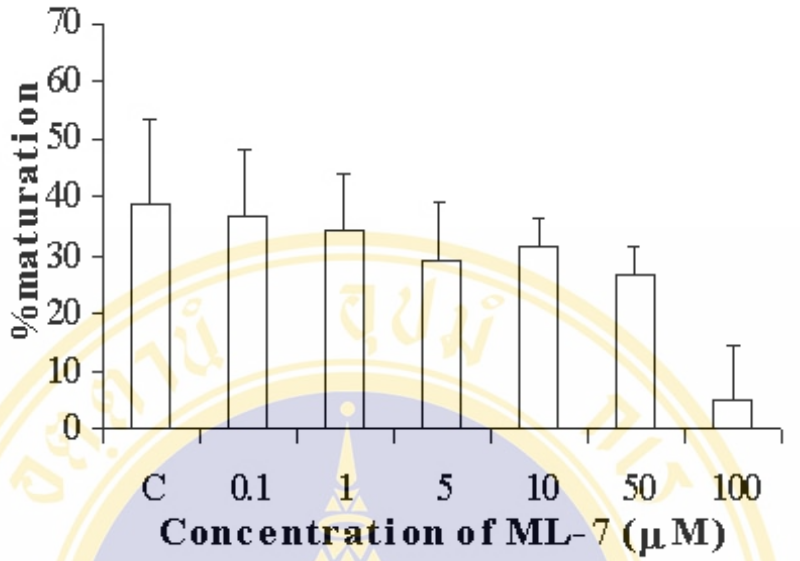

B.

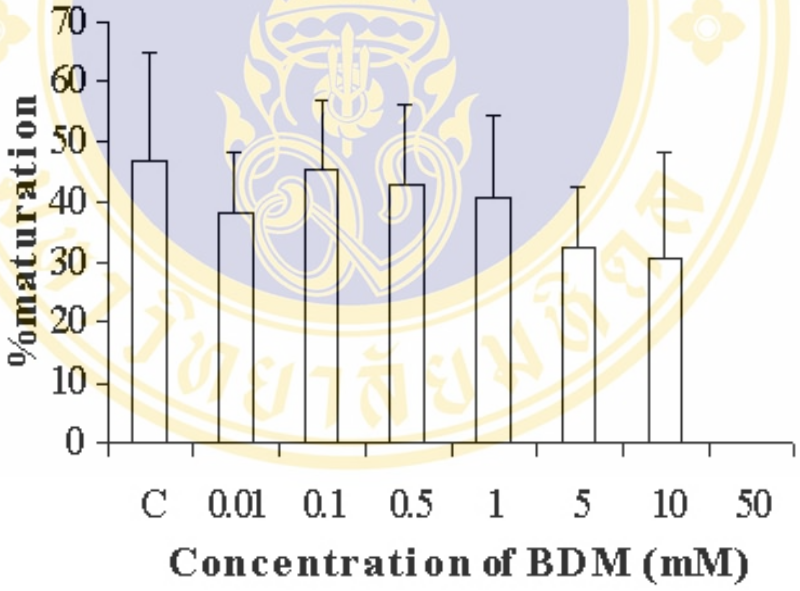

Figure 13 Effect of ML-7 (A) and BDM (B) on maturation of schizont. Trophozoite-infected erythrocytes at 2% hematocrit and 3% parasitemia were exposed to the inhibitor for 16-20 h before the number of schizont-infected erythrocyte per 5,000 erythrocytes in Giemsa-stained thin blood films were counted under microscope. Schizonts with more than 5 nuclei were scored and expressed as percentage relative to control. Control culture was exposed to solvents in the absence of inhibitor. The results shown represented mean±S.D from three independent experiments, each carried out in triplicate.

4.4 Effect of myosin II inhibitors on parasite development from schizont stage to ring stage

In order to complete the life cycle, schizonts further mature and rupture into free-moving 'merozoites'. These soon invade naive erythrocytes nearby to become once again, ring-stage parasites. The myosin II inhibitors were examined whether they played a role during these steps by exposing schizonts to the inhibitors for 12-18 h before scoring for ring-stage erythrocytes.

Both ML-7 and BDM inhibited ring-stage formation in a dose-dependent manner, showing IC_{50} value of 31.9±1.7 μM and 5.4±1.2 mM, respectively (Figure 14A & B). However, when the number of remaining schizonts were scored, the results were different between the two inhibitors. With increasing concentrations of ML-7, the number of ring-stage parasite decreased in a dose-dependent manner while the number of schizont remained low and relatively unchanged throughout. In contrast, increasing concentrations of BDM caused a dose-dependent decrease of ring-stage parasites concomitant with an increase in schizont accumulation over the concentration range of 1-10 mM. Above 10 mM BDM, the number of residual schizonts was minimal and merozoite invasion was inhibited by 94 % (Figure 15A & B).

A.

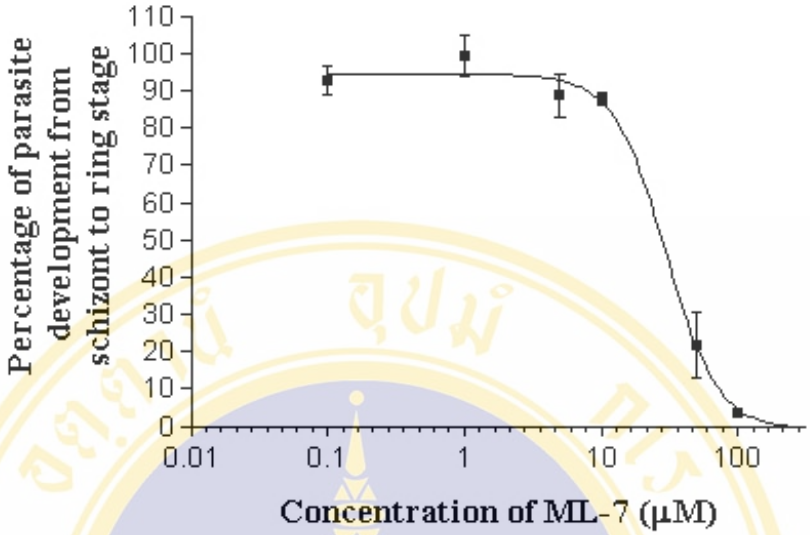

B.

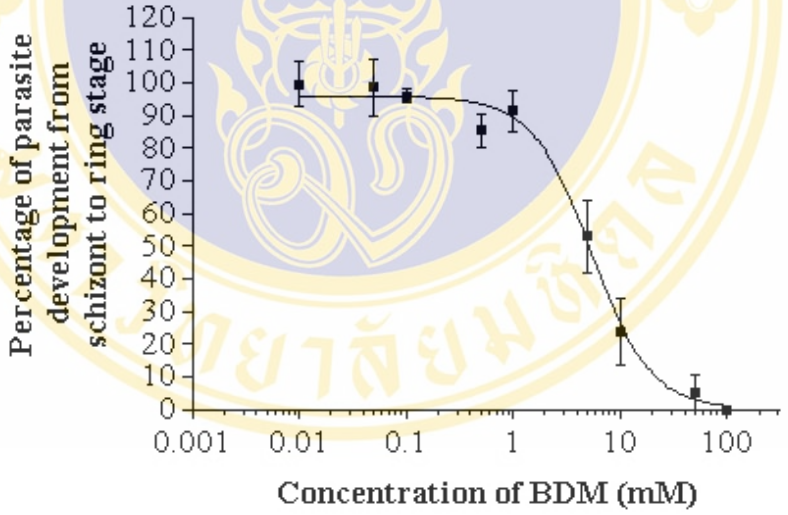

Figure 14 Effect of ML-7 (A) and BDM (B) on *P. falciparum* development from schizont to ring stage. Schizont-infected erythrocytes at 2% hematocrit and 5% parasitemia were exposed to the inhibitor for 12-18 h before parasitemia were determined by counting 1,000 erythrocytes in Giemsa-stained thin blood films under microscope. The results shown represented mean±S.E.M of percentage of number of ring relative to control from three independent experiments, each carried out in triplicate. Control cells were exposed to the solvents in the absence of inhibitor.

A.

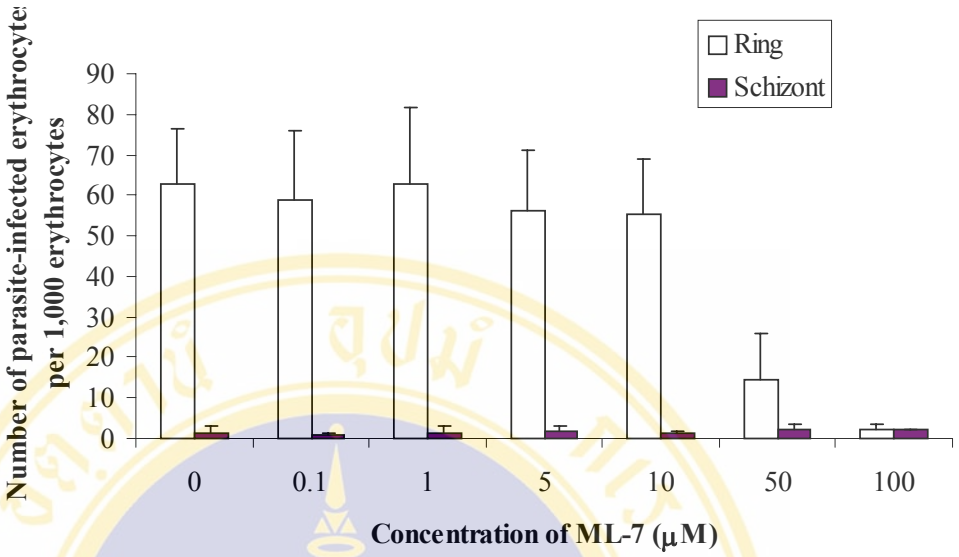

B.

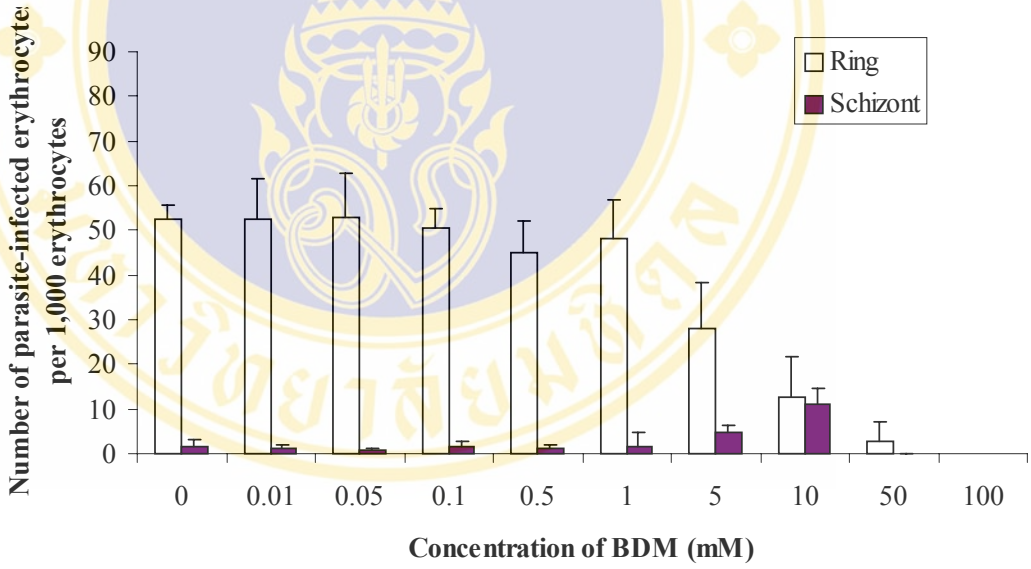

Figure 15 Effect of ML-7 (A) and BDM (B) on schizont accumulation. Schizont-infected erythrocytes at 2% hematocrit and 5% parasitemia were exposed to the inhibitor for 12-18 h before the parasite at different stage in 1,000 erythrocytes were counted in Giemsa-stained thin blood films under microscope. The results shown represented mean±S.D three independent experiments, each carried out in triplicate. Control cells were exposed to the solvents in the absence of inhibitor.

Table 3 Summary of IC_{50} value of ML-7 and BDM on different stages of *P. falciprum* development *in vitro*

	Ring to schizont	**Ring to trophozoite**	**Trophozoite to schizont**	**Schizont to ring**
ML-7 (μM)	6.3±1.1	4.6±1.3	43.5±1.3	31.9±1.7
BDM (mM)	6.4±1.1	17.0±1.4	10.6±1.2	5.4±1.2

4.5 Observation of morphology of *P. falciparum* parasites after exposure to myosin II inhibitors

4.5.1 Normal *P. falciparum* in *in vitro* continuous culture

Normally, in continuous culture, ring stage parasites were characterized by violet-stain nuclei and thick rim of blue cytoplasm (Figure 16A). After 20-24 h, the ring stage developed to trophozoite stage, in which the blue cytoplasm expanded to occupy 1/3-1/2 of the erythrocyte volume. An enlarged violet nucleus and the brown pigment granules become visible (Figure 16B). Sixteen to twenty hours after that, the parasite developed to schizont stage, of which the cytoplasm further expanded and the multiple nuclei become distinct. The brown pigments were also present at this stage. Then each nucleus migrated to the periphery of the parasite cytoplasm forming a merozoite. The immature schizont had 2-5 nuclei (Figure 16C) whereas those with mature schizont had more than 5 nuclei (Figure 16D). Typically schizonts can undergo multiple rounds of nuclear division, gave rise up to 16-20 nuclei (13). After erythrocyte rupture, the merozoites were released into culture and some invaded naive erythrocytes to form ring stage of the new developmental cycle (Figure 16E).

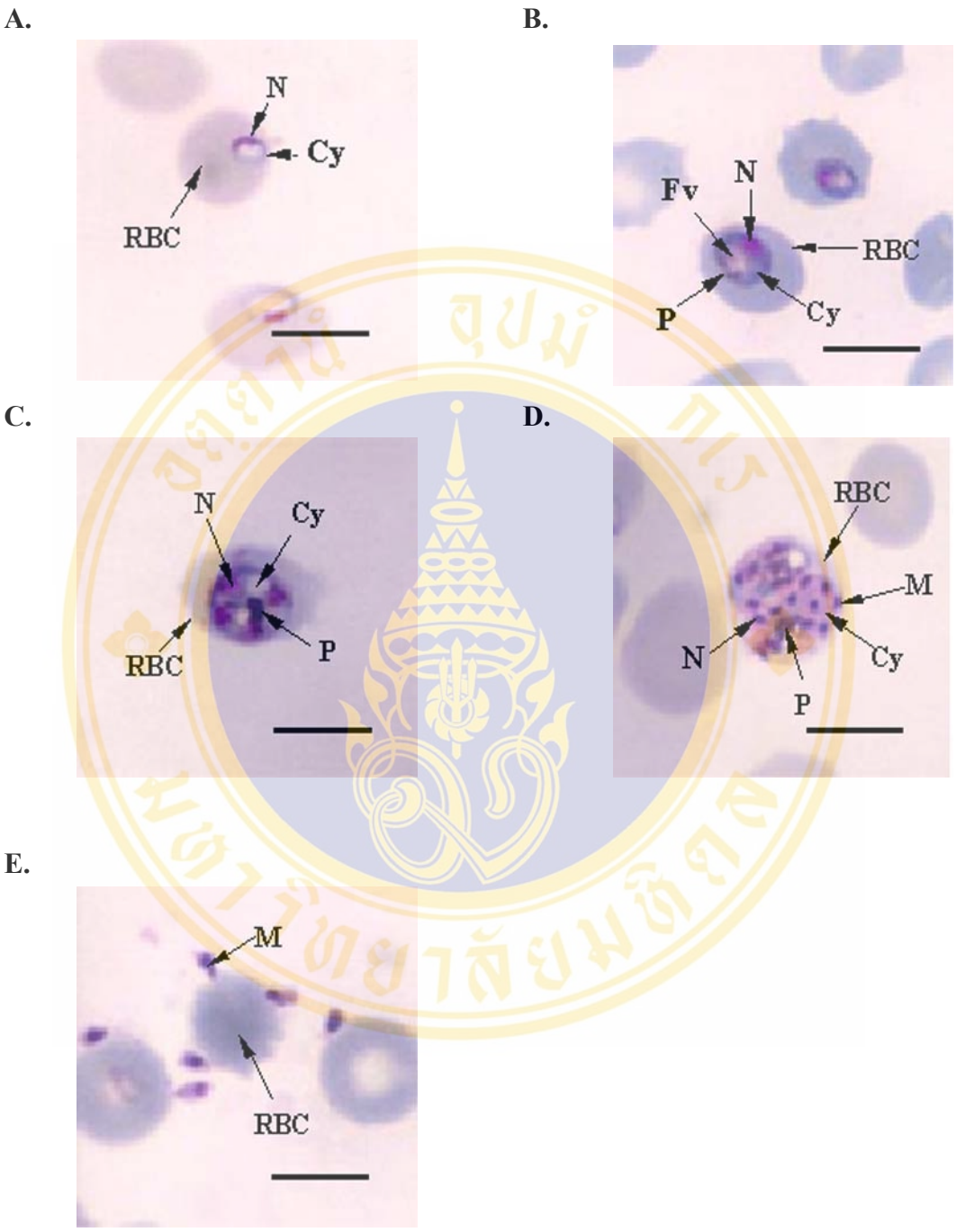

Figure 16 Normal *P. falciparum* in *in vitro* continuous culture. The figure shows (A) ring-, (B) trophozoite-, (C) immature schizont-, (D) mature schizont- and (E) merozoite stage parasite. Bar = 7 μm. (N: nucleus, Cy: cytoplasm, Fv: food vacuole, P: brown pigment, M: merozoite and RBC: erythrocyte)

4.5.2 Effect of myosin II inhibitors on *P. falciparum* development from ring stage to trophozoite stage.

4.5.2.1 Effect of ML-7 on *P. falciparum* development from ring stage to trophozoite stage.

In the presence of 1 μM of ML-7, the parasites developed from ring to normal-looking trophozoites as in control (Figure 17A). At 5 μM of ML-7 (Figure 17B), with incomplete inhibition, some dead parasites were observed. These were characterized by rough edges and poorly defined nuclear-cytoplasmic boundaries. The brown pigments still occurred. At 10 μM of ML-7 (Figure 17C), the parasite cytoplasm was enlarged with a rough edge which was difficult to locate. The brown pigments did not occur in this condition. The nucleus condensed and parasite still had a food vacuole. At 50 μM of ML-7 in Figure 17D showed two parasites that remained at ring stage with condensed nucleus, and their cytoplasm was not enlarged. At 100 μM of ML-7 where complete inhibition was observed, all parasites were inhibited at ring stage. Most of the dead parasites showed pyknotic nuclei without cytoplasm. These are presumably dead parasites (Figure 17E). However, at 100 μM of ML-7, the erythrocytes exhibited a larger center paler than the erythrocytes in control well. At concentrations below 100 μM, ML-7 did not significantly affect the erythrocyte morphology.

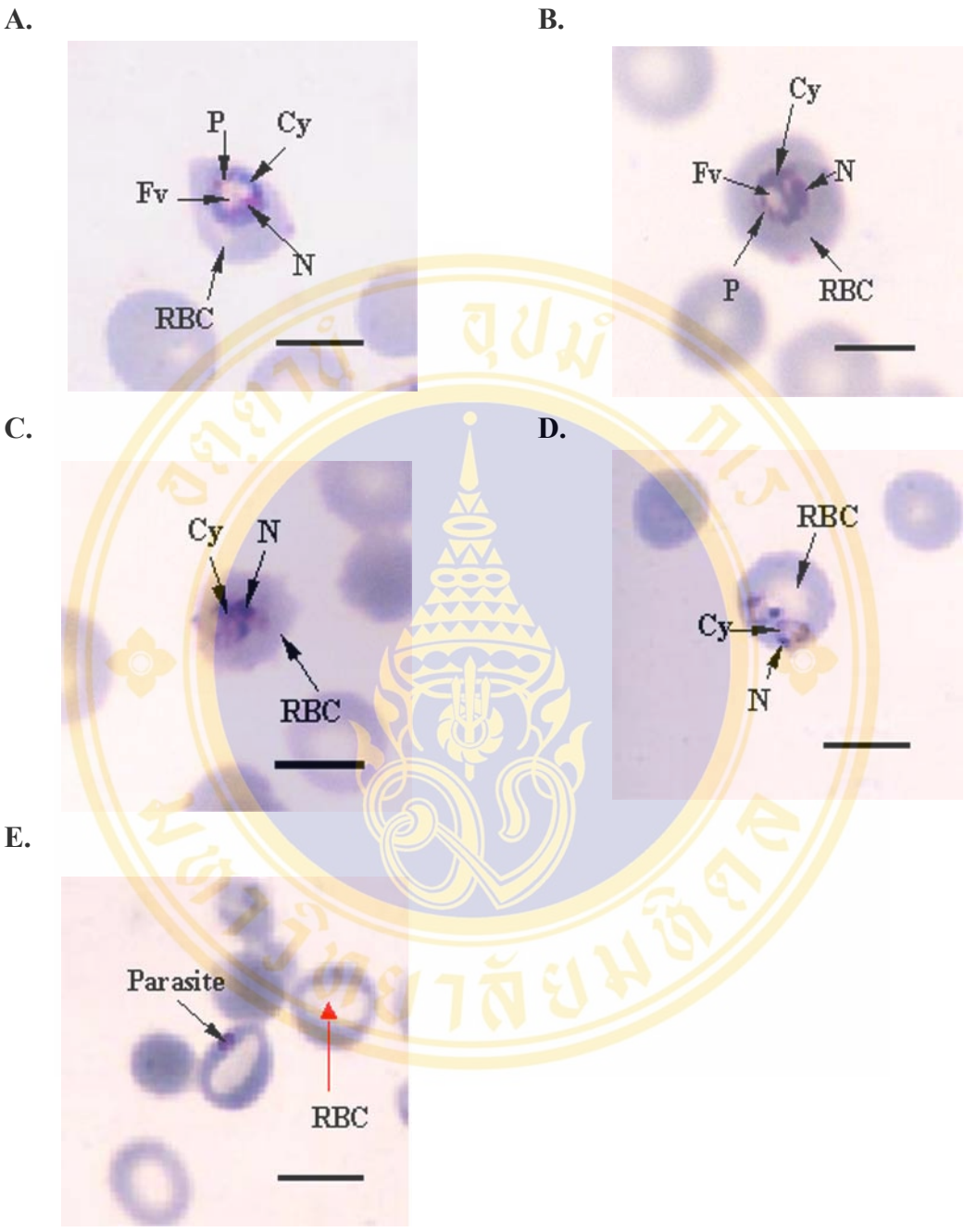

Figure 17 Effect of ML-7 on *P. falciparum* development from ring to trophozoite stage. Ring-infected erythrocytes were incubated at 37 ^{o}C for 22-24 h in the presence of ML-7 before the Giemsa-stained thin blood films were made and the phenotypes scored. (A) 1 μM ML-7, (B) 5 μM ML-7, (C) 10 μM ML-7, (D) 50 μM ML-7 and (E) 100 μM ML-7. Bar = 7 μm. (N: nucleus, Cy: cytoplasm, Fv: food vacuole, P: brown pigment, and RBC: erythrocyte)

5.2.2 Effect of BDM on *P. falciparum* development from ring stage to trophozoite stage.

At 1 and 5 mM of BDM, the parasites developed normally as in control (Figure 18A & B). At 10 mM of BDM, most of the parasites developed to the normal trophozoite, although they are smaller than control (not shown). The dead trophozoite was characterized by its small size and the nucleus could not be distinguished from the cytoplasm and it was difficult to see the brown pigment (Figure 18C). At 50 mM of BDM (Figure 18D), where complete inhibition of development was observed, all parasites were inhibited at ring stage. They appeared as pyknotic nuclei without cytoplasm. These are presumably dead parasites. The non-infected erythrocytes in all concentrations of BDM were normal.

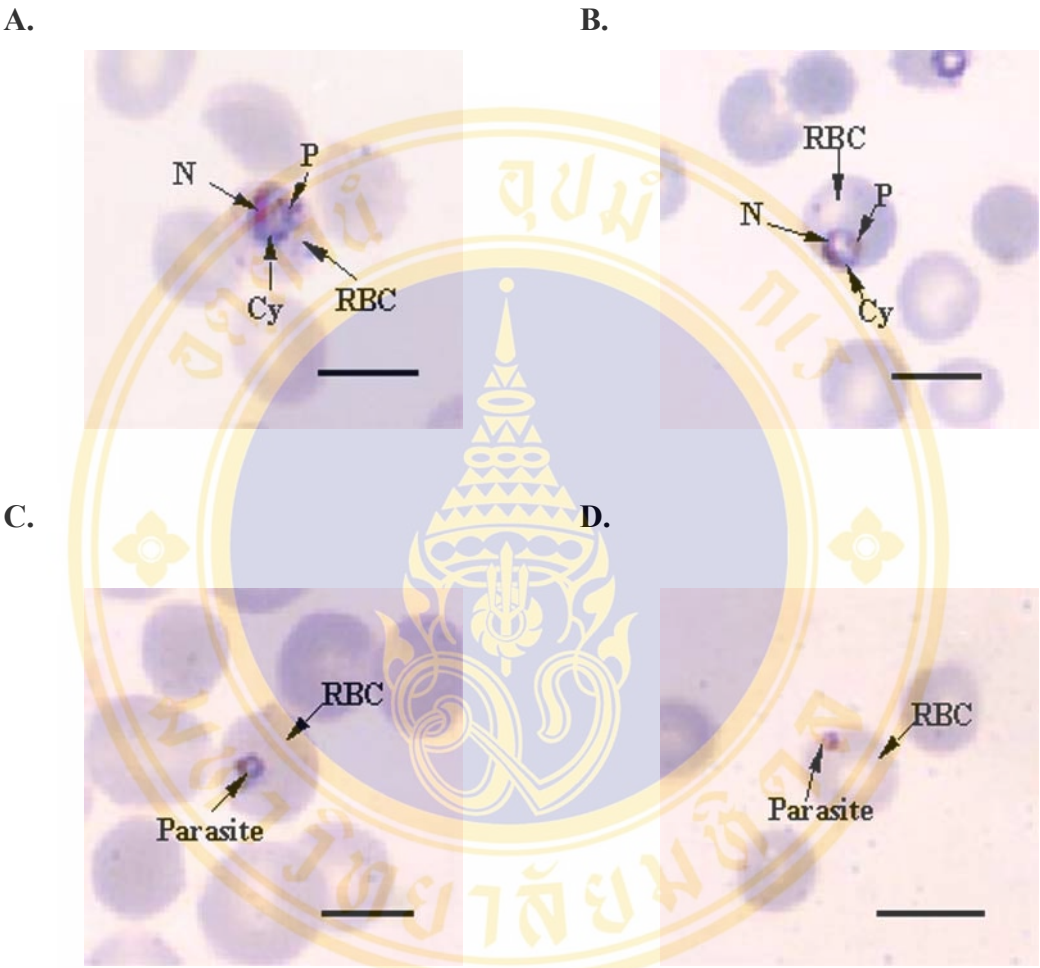

Figure 18 Effect of BDM on *P. falciparum* development from ring to trophozoite stage. Ring-infected erythrocytes were incubated at 37 ^{o}C for 22-24 h in the presence of BDM before the Giemsa-stained thin blood films were made and the phenotypes scored. (A) 1 mM BDM, (B) 5 mM BDM, (C) 10 mM BDM, and (D) 50 mM BDM. Bar = 7 μm. (N: nucleus, Cy: cytoplasm, Fv: food vacuole, P: brown pigment, and RBC: erythrocyte)

4.5.3 Effect of myosin II inhibitors on *P. falciparum* development from trophozoite stage to schizont stage.

4.5.3.1 Effect of ML-7 on *P. falciparum* development from trophozoite stage to schizont stage

After 16-20 h of incubation, parasite develop to schizont stage. In the presence of 0.5 μM of ML-7, the parasite developed normally (Figure 19A). At 5 μM of ML-7, most of the parasites developed to normal schizont, but vacuolated cytoplasm began to appear (Figure 19B). At 10 μM of ML-7, dead schizont developed vacuolated cytoplasm and the number of nuclei was less than in control (Figure 19C). At 50 μM of ML-7, most of the parasites failed to develop and dead trophozoite appeared with increased size and a vacuolated cytoplasm (Figure 19D). At 100 μM of ML-7, the dead trophozoites shrank as dense particles as shown in Figure 19E. However, at 100 μM of ML-7, the erythrocytes exhibited a larger center paler than the erythrocytes in control well. At concentrations below 100 μM, ML-7 did not significantly affect the non-infected erythrocyte morphology.

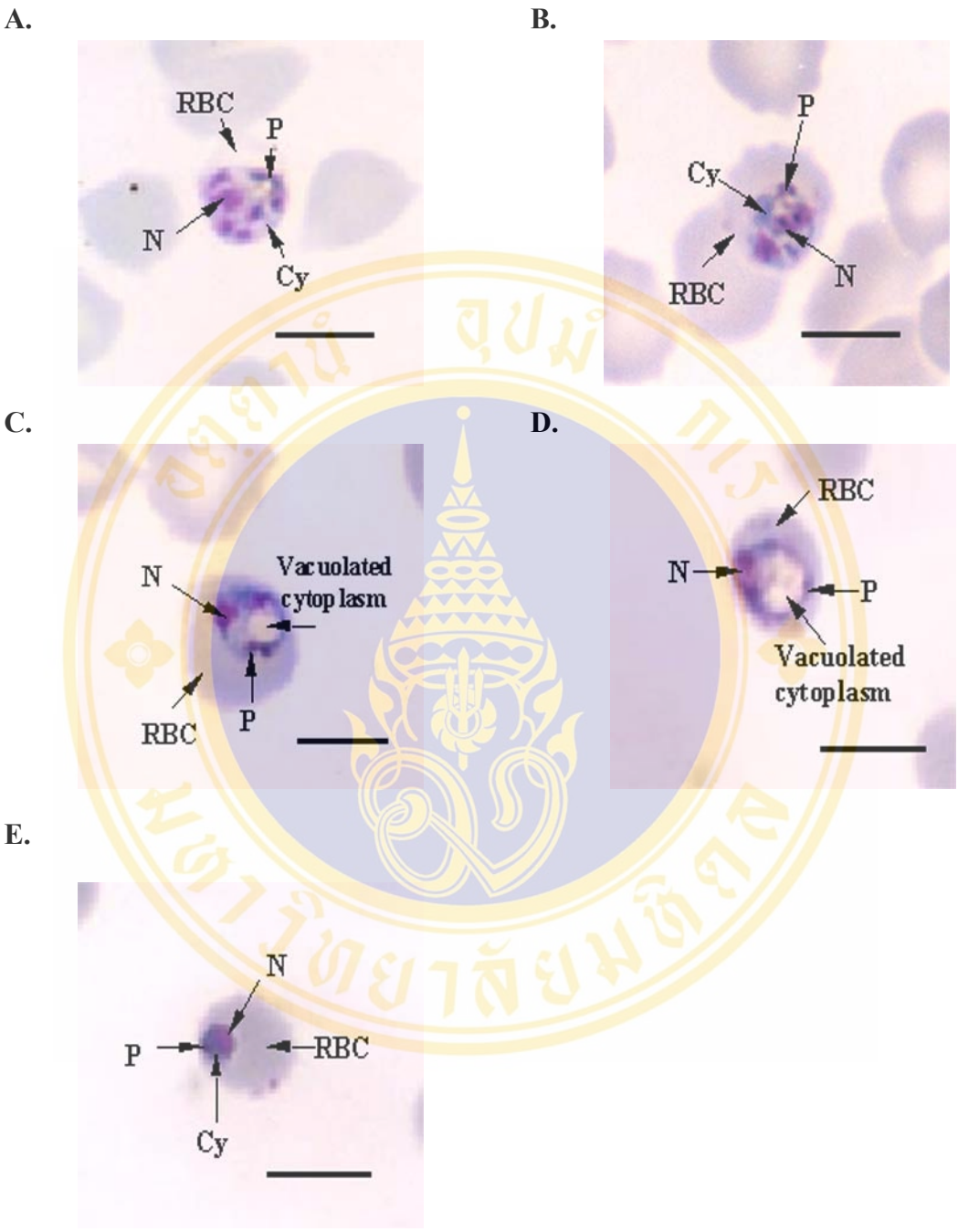

Figure 19 Effect of ML-7 on *P. falciparum* development from trophozoite to schizont stage. Trophozoite-infected erythrocytes were incubated at 37 ^{o}C for 16-20 h in the presence of ML-7 before the Giemsa-stained thin blood films were made and the phenotypes scored. (A) 0.5 μM ML-7, (B) 5 μM ML-7, (C) 10 μM ML-7, (D) 50 μM ML-7 and (E) 100 μM ML-7. Bar = 7 μm. (N: nucleus, Cy: cytoplasm, Fv: food vacuole, P: brown pigment, and RBC: erythrocyte)

4.5.3.2 Effect of BDM on *P. falciparum* development from trophozoite stage to schizont stage

After 16-20 h incubation, in the presence of 1 mM of BDM, trophozoites developed to normal schizonts (Figure 20A). At 5 mM of BDM, the abnormal schizonts which had fragmented nuclei were observed (Figure 20B). At 10 mM of BDM, which is incomplete inhibitory concentration. Some of the parasite developed to schizont but some of them dead at trophozoites which shrank without multiple nuclei (Figure 20C). At 50 mM of BDM, dead trophozoites had shrunken residue bodies as shown in Figure 20D. The non-infected erythrocytes in every concentration of BDM were normal as in control.

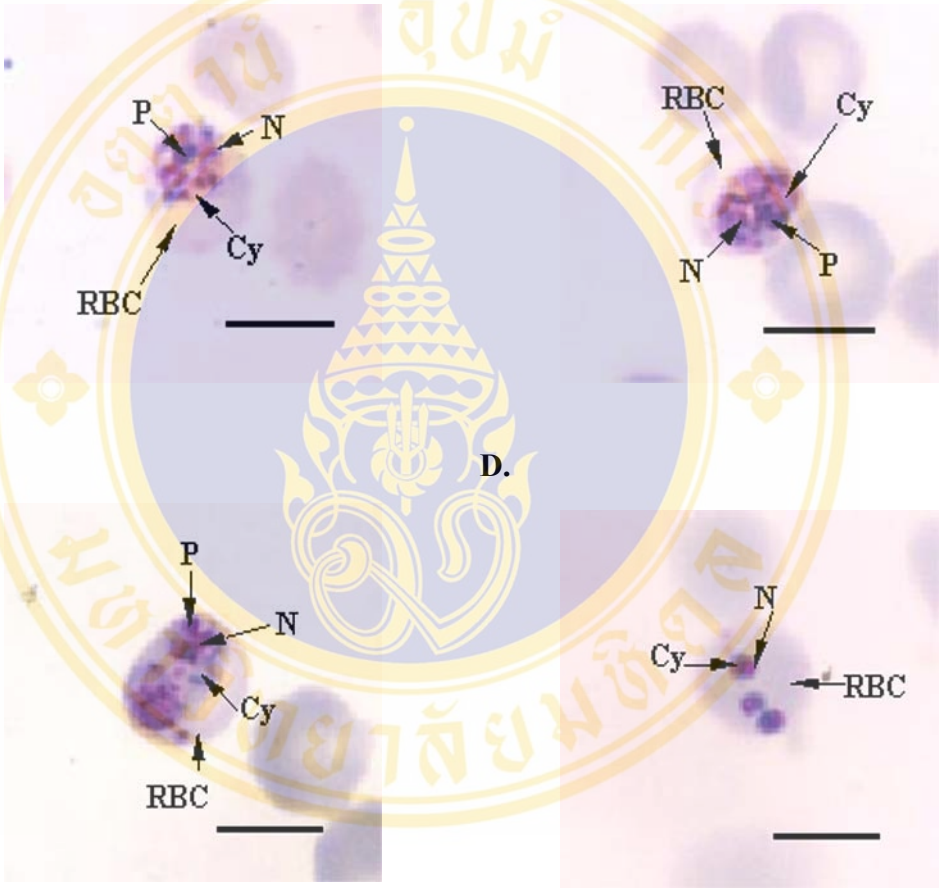

Figure 20 Effect of BDM on *P. falciparum* development from trophozoite to schizont stage. Trophozoite-infected erythrocytes were incubated at 37 ^{o}C for 16-20 h in the presence of BDM before the Giemsa-stained thin blood films were made and the phenotypes scored. (A) 1 mM BDM, (B) 5 mM BDM, (C) 10 mM BDM and (D) 50 mM BDM. Bar = 7 μm. (N: nucleus, Cy: cytoplasm, Fv: food vacuole, P: brown pigment, and RBC: erythrocyte)

4.5.4 Effect of myosin II inhibitors on *P. falciparum* development from schizont stage to ring stage.

4.5.4.1 Effect of ML-7 on *P. falciparum* development from schizont stage to ring stage

After 12-18 h of incubation, the presence of 1 μM of ML-7, parasite morphology looked normal as in control (Figure 21A). At 10 μM of ML-7, number of ring-infected erythrocytes and also morphology was same as in control, although there were some abnormal schizonts (Figure 21B). At 50 μM of ML-7, dead schizonts with shrunken nuclei were apparent with rough edge (Figure 21C). At 100 μM of ML-7, dead schizonts with round dense particles were seen. The dead schizont edge was determined with difficulty, at this concentration, some of infected erythrocytes lysed and there were the parasites located outside the erythrocyte (Figure 21D) and erythrocytes had a larger center paler compared to erythrocytes in control well. The non -infected erythrocytes exposed to ML-7 at concentration lower than 100 μM were normal.

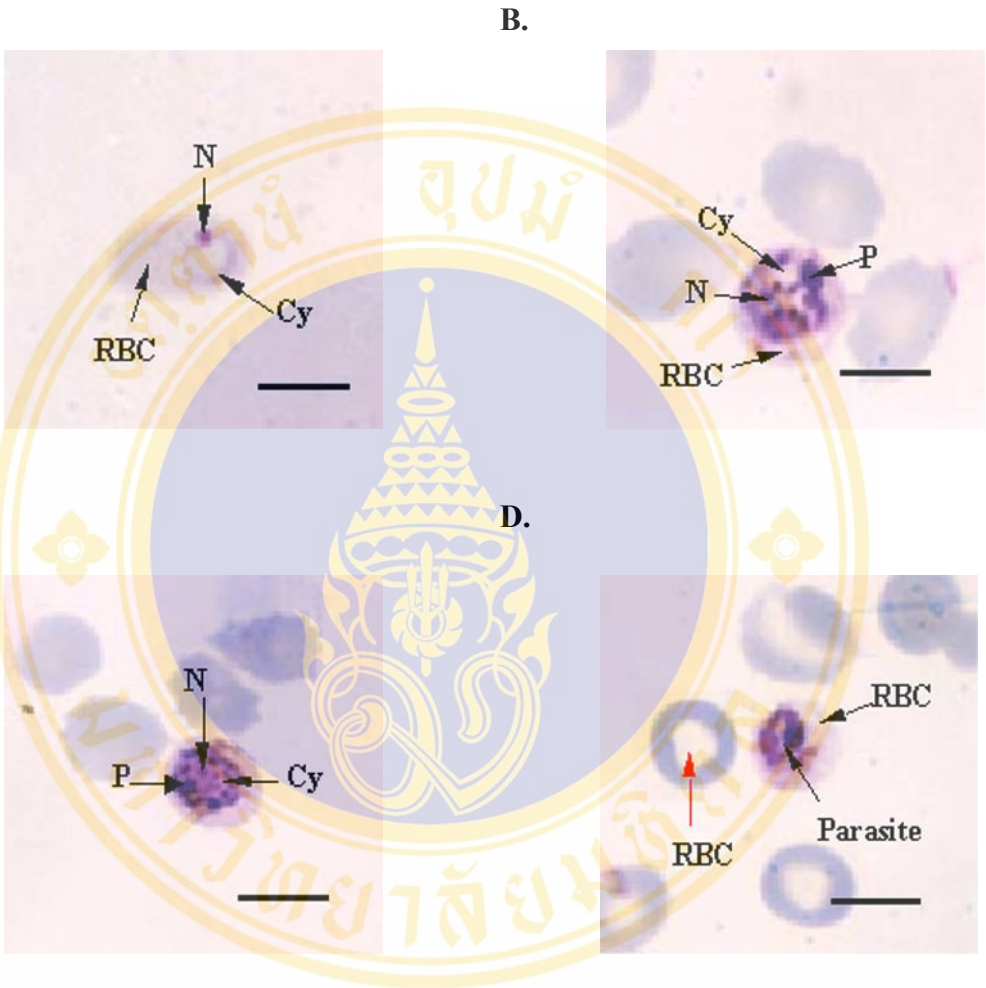

Figure 21 Effect of ML-7 on *P. falciparum* development from schizont to ring stage. Schizont-infected erythrocytes were incubated at 37 ^{o}C for 12-18 h in the presence of ML-7 before the Giemsa-stained thin blood films were made and the phenotypes scored. (A) 1 μM ML-7, (B) 10 μM ML-7, (C) 50 μM ML-7 and (D) 100 μM ML-7. Bar = 7 μm. (N: nucleus, Cy: cytoplasm, Fv: food vacuole, P: brown pigment, and RBC: erythrocyte)

4.5.4.2 Effect of BDM on *P. falciparum* development from schizont stage to ring stage.

After 12-18 h exposed to 1 and 5 mM of BDM, normal rings and schizonts were seen (Figure 22A & B). At 10 mM of BDM, dead schizonts with shrunken nuclei which failed to distribute throughout the cytoplasm were apparent (Figure 22C). At 50 mM of BDM, these schizonts appeared as round dense particles (Figure 22D), at this concentration, some of the infected erythrocyte lysed and there were the parasites located outside the erythrocytes. The non-infected erythrocytes exposed to all concentrations of BDM were normal as in control.

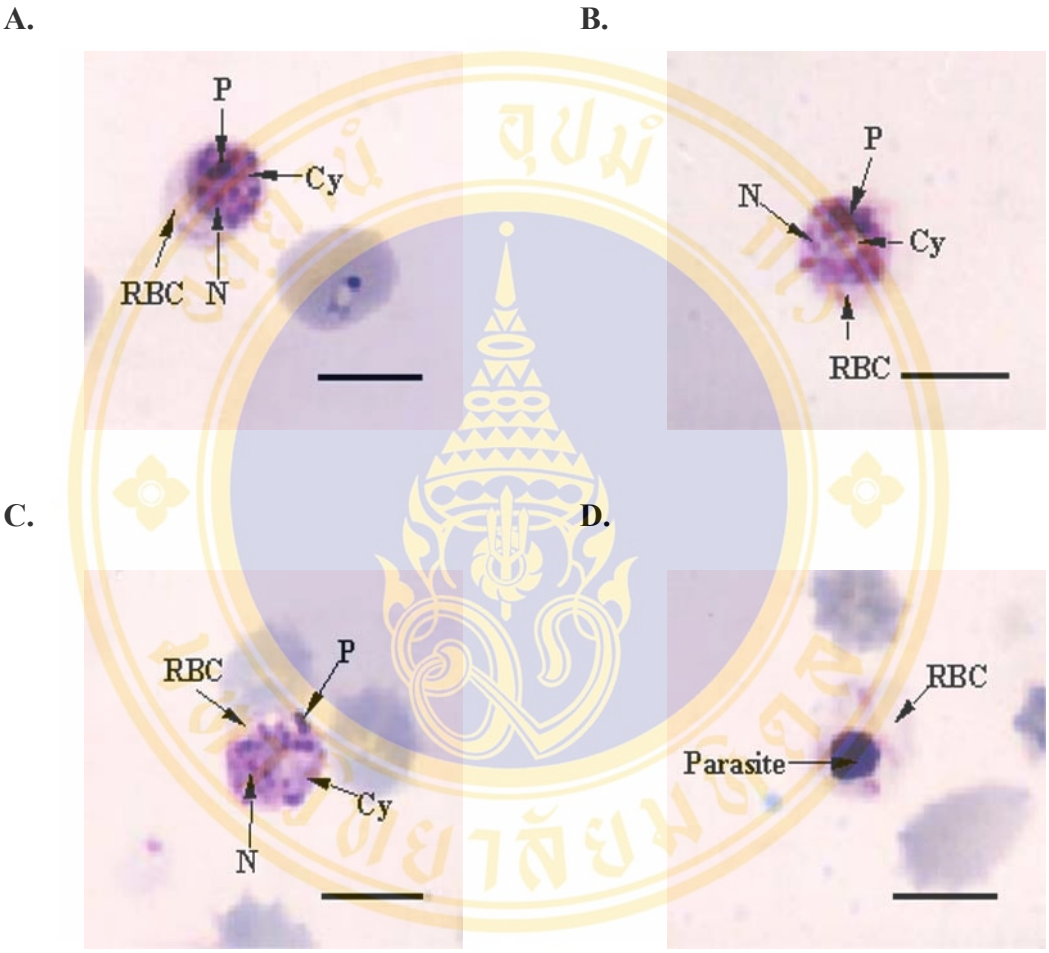

Figure 22 Effect of BDM on *P. falciparum* development from schizont to ring stage. Schizont-infected erythrocytes were incubated at 37 ^{o}C for 12-18 h in the presence of BDM before the Giemsa-stained thin blood films were made and the phenotypes scored. (A) 1 mM BDM, (B) 5 mM BDM, (C) 10 mM BDM and (D) 50 mM BDM. Bar = 7 μm. (N: nucleus, Cy: cytoplasm, Fv: food vacuole, P: brown pigment, and RBC: erythrocyte)

4.6 Effect of combination of myosin II inhibitors on *P. falciparum* growth

Normally, myosin is regulated in a sequential manner: myosin light chain is phosphorylated by myosin light chain kinase (MLCK), and activated myosin ATPase in turns interactions with actin. The mechanism of regulation of *P. falciparum* myosin is still not clear. Therefore, the effects of the myosin inhibitors on anothers were examined. Parasite growth was monitored using (^{3}H) hypoxanthine uptake. When sub-inhibitory concentrations of BDM (0.006, 0.024, 0.098, 0.391 and 1.563 mM) were present in the parasite cultures, there were no effects on IC_{50} values of ML-7 (Figure 23A), whereas, presence of sub-inhibitory concentrations of ML-7 (0.006, 0.024, 0.098, 0.391 and 1.563 μM) antagonized (ie. raised IC_{50} values) of BDM (Figure 23 B).

A.

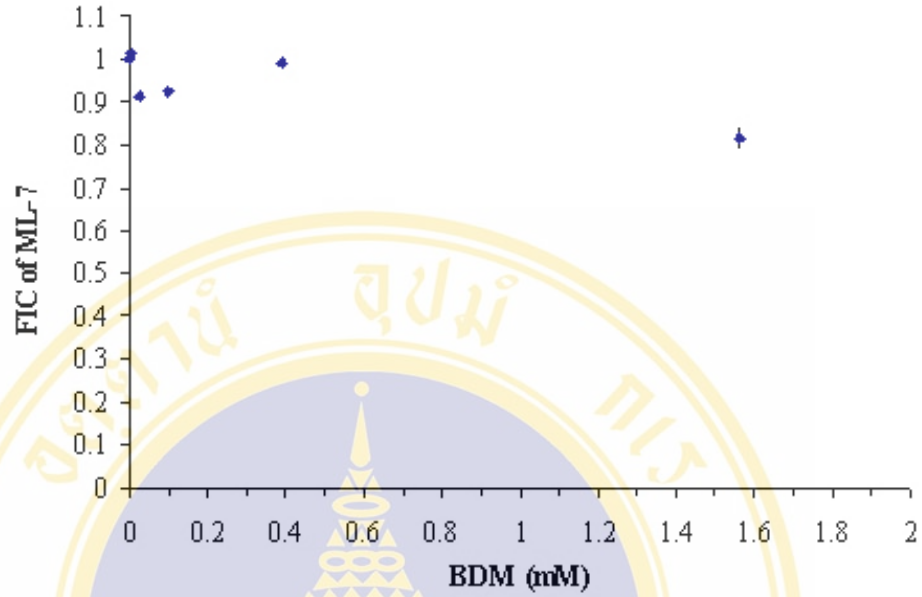

B.

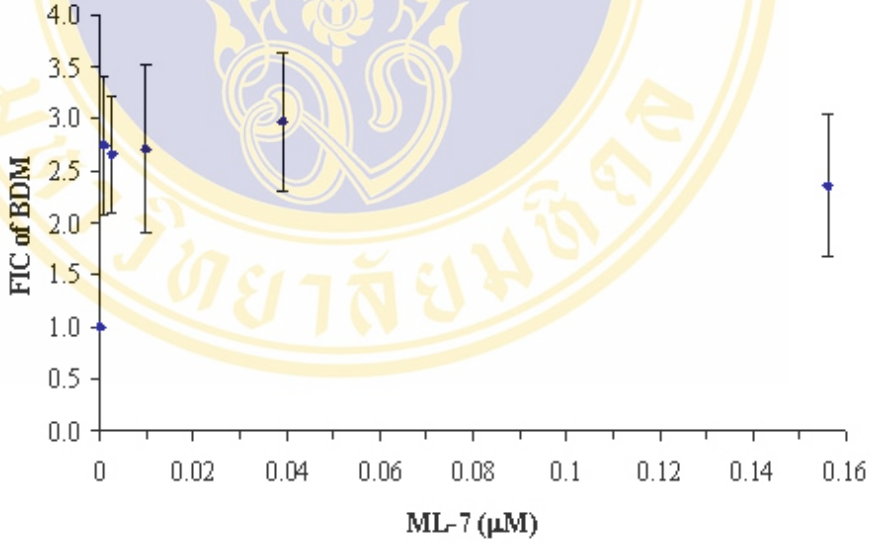

Figure 23 Effects of the combination of myosin inhibitors on *P. falciparum* growth *in vitro*. Parasite growth was monitored using (^{3}H) hypoxanthine uptake. (A) The inhibitory effects of myosin II inhibitor BDM at sub-inhibitory concentrations (0.006, 0.024, 0.098, 0.391 and 1.563 mM), on IC_{50} values of ML-7. (B) the inhibitory effect of ML-7 at sub-inhibitory concentrations (0.006, 0.024, 0.098, 0.391 and 1.563 µM) on IC_{50} values of BDM.

CHAPTER 5
DISCUSSION

Myosin in erythrocyte is classified as type II that can form bipolar filaments. The presence in erythrocytes of calmodulin and myosin light chain kinase rise the possibility that, as non-muscle myosin II, erythrocyte myosin is regulated by phosphorylation of myosin light chain, and this stimulates the actin-activated ATPase. It found to interact with spectrin-actin-protein 4.1 complexes, where force might be transmitted to the membrane skeleton, this has led to the suggestion that erythrocyte shape changes might be mediated by an ATP-dependent actin-myosin contractile mechanism.

After invasion, the ring stage parasite begins to feed on the surrounding erythrocyte. The ring eventually changes shape to a more rounded or irregular trophozoite. As the parasite grows, the area of the PVM surrounding it also increases. Both ring and trophozoite feed on the erythrocyte and gradually alter it by exporting various parasite proteins into its cytoplasm and to its surface. Some of these proteins produce small angular elevations (knobs) on the erythrocyte surface causing erythrocytes infected with more mature stages to become even less deformable than ring forms. Erythrocytes start to change its shape and deformability. The parasite then undergoes replicative nuclear division to reach schizont stage. Export of parasite proteins into the erythrocyte continues until late in the life of the schizont. As the exported parasite proteins distort the cytoskeleton and membrane of the cell, in addition to increasing the numbers of knobs at its surface which make the surface of the erythrocyte becomes quite angular in profile. Finally, the schizont rupture and merozoites release to blood stream.

There are four types of *P. falciparum* myosin: Pfmyo-A, Pfmyo-B, Pfmyo-C and Pfmyo-D. The expression Pfmyo-B, Pfmyo-C and Pfmyo-D have not been report. Pfmyo-A is located between the parasite membrane and cisternal membrane and

located predominantly towards the apex. Its first appearance is in the schizont and vanishes after invasion. It presents in the right place and at the right time, and is now thought to play role in merozoite entry into erythrocyte.

The goal of this thesis was, thus, to investigate the role of myosin-based contractile system of *P. falciparum* and host red cell during parasite growth within the erythrocyte, and in the invasion process, by assessing the effects of myosin inhibitors, BDM and ML-7, on parasite intracellular development and invasion.

5.1 Action of BDM and ML-7

BDM inhibits myosin ATPase. It have phosphatase activity which was shown to be relatively selective; that is, the potency for interacting with various phosphate molecules was phosphotriesters>phosphomonoesters>phosphodiesters (55). While the concentrations of BDM are required relatively high, they are entirely consistent with the effects of this inhibitor on myosin specific functions in higher eukaryotic cells. It blocks myosin II-based cell motility in PtK2 cells and myosin Ic-based contractile vacuole function in *Acanthamoeba.* At 10 mM it inhibits the ATPase activity of purified myosin V (to 13.8% of control), human platelet myosin II (to 5.1% of control) and of a *Drosophila* protein fraction (to 26.6% of control)(45). Treatment of polymorphonuclear leucocyte (PMN) causes shape change and inhibits colchicine-induced locomotion with IC_{50} of 8 and 15.5 mM BDM, respectively (56). In normal rat kidney (NRK) cell, BDM at 20 mM was found to inhibit brefeldin A (BFA)-induced Golgi disassembly without alteration in calcium homeostasis (57). In each of these examples, myosins act as molecular motors to generate force by moving along actin filaments. BDM has also been shown to affect calcium release from the sarcoplasmic reticulum (in particular when it is used at higher concentrations of 30 mM) (58).

ML-7 is myosin light chain kinase inhibitor. a potent and selective inhibitor of MLCK. This compound inhibits both Ca^{2+}-calmodulin dependent and independent smooth muscle myosin light chain kinase to a similar extent, and its inhibition is of the competitive type with respect to ATP-binding site on the kinase molecule (44). Ki values for myosin light chain kinase (MLCK) and other kinases are shown in Table 2.

At 20 μM ML-7 did not alter calcium homeostasis of normal rat kidney (NRK) cell but at 30 μM ML-7, the Golgi complex was perinuclear, instead of showing its continuous reticular shape characteristic of untreated NRK cells (57). ML-7 at 20 μM reduces cell viability (after 16 h of exposure) of pancreatic cancer cell line (MIA PaCa-2 and BxPC3) to about 80% of control. In contrast, up to 40 μM ML-7 did not reduce that of Panc1 cell significantly (59) and up to 75 μM ML-7 had virtually no effect on survival of MLL cells during 6 h of treatment (60).

5.2 Which stage of development was effected by the inhibitors?

Myosin II is regulated by myosin light chain kinase (MLCK) and myosin ATPase activity. BDM can inhibit ATPase activity of many kinds of myosin at millimolar concentration. From data of ^{3}H-hypoxanthine incorporation assay, BDM inhibited growth of the parasite from ring to schizont stage with IC_{50} value of 6.4 mM. After examination whether which particular stage of development was affected by BDM, we found that BDM could inhibit development at every stage (ring to trophozoite, trophozoite to schizont, and schizont to ring) at similar concentrations. So the inhibitory effect of BDM on parasite growth is effective at both the intraerythrocytic stages of development and at the invasion step as well. Development from schizont to ring stage (invasion step) gave the lowest IC_{50} value (5.4 mM); this may be because the merozoite has a chance to be exposed to the inhibitor directly. Taken altogether, the BDM inhibition data suggest that active myosin is required for every stage of parasite development.

The other myosin inhibitor used, ML-7, is the myosin light chain kinase inhibitor. Using the ^{3}H-hypoxanthine incorporation assay, ML-7 inhibited growth of the parasite from ring to schizont at low concentration (IC_{50}=6.3 μM). After examination whether which particular stage of development was affected by ML-7, we found that ML-7 inhibited development from ring to trophozoite stage at μM concentration, whereas development of trophozoite to schizont stage, schizont maturation and from schizont to ring stage (schizont rupture and merozoite invasion step), required 10 fold more inhibitor. In addition, increasing concentrations of ML-7

cause a does-dependent decrease of number of ring while number of schizont remained low and relatively unchanged throughout. This data implied that both schizont rupture and merozoite invasion do not require a ML-7-sensitive MLCK. Thus, development of ring to trophozoite stage in parasite intraerythrocyteic growth requires a ML-7-sensitive MLCK.

As described earlier, myosin II function requires phosphorylation of myosin light chain kinase by MLCK, which then stimulates actin-activated myosin ATPase activity. From data using the inhibitor BDM, showed that myosin ATPase activity is required during all stages of malaria parasite intraerythrocytic growth and development. In addition, increasing concentration of BDM that caused number of ring decreased concomitant with an increase in schizont accumulation implied that schizont rupture and probably merozoite invasion require myosin ATPase activity. However, phosphorylation by ML-7-sensitive MLCK appeared to take place during the early stage of intraerythrocytic growth, i.e. from ring to trophozoite stage. One can explain that development of malaria parasite at the later stages, including invasion, requires another species of MLCK that is less sensitive to ML-7, or that these late stages of parasites use a different form of myosin that require phosphorylation by ML-7-insensitive MLCK but itself is still sensitive to inhibition by BDM. Another explanation, but less likely, is that uptake of ML-7 by the parasite late stages is impaired compared to the early ring stage.

5.3 Do the inhibitors affect myosin of parasite or erythrocyte?

Development from ring to trophozoite may require myosin II function. Myosin II is detected in erythrocyte but there has been no report of myosin II in parasite. During development from ring to trophozoite stage, as the ring enlarges, it begins to synthesize molecules specific to this stage (ring-infected erythrocyte surface antigen (RESA), ring surface protein 1 (RSP-1), ring surface protein 2 (RSP-2)) (61) and PfEMP1, exporting some of them into the erythrocyte, and modifying the erythrocyte membrane which now begins to adhere to the linings of visceral and other blood vessels, including those of the placenta (6). The ring eventually grows into trophozoite which have active feeding, growth and erythrocyte modification (knobs).

Maurer's cleft is developed. The area of the PVM surrounding it also increases and there is tubovesicular network formation to increase the parasite access to food. Movements of vesicles between PVM and Maurer's clefts remains mysterious. There is evidence for erythrocyte myosin II binding to isolated Golgi accompanied by the recruitment of actin. Immunoelectron microscopy showed that erythrocyte myosin II is associated with the PVM and the Maurer's clefts (62). So erythrocyte myosin II might move along actin filaments to either pull a vesicle bud or to move vesicles away from the PVM and across the erythrocyte cytosol. Blocking of erythrocyte myosin II may disrupt this process.

In addition, the inhibitors may affect parasite myosin. During development from ring to trophozoite stage there are increase in transcription and translation. Data from DeRisi *Plasmodium falciparum* HB3 time course microarray of a putative myosin similar to *Plasmodium falciparum* myosin pfmyo-c (14) showed that expression of this kind of parasite mRNA myosin begins in early ring stage and is highly expressed in late trophozoite stage, and after that gradually decreases until the end of parasite cycle. From Table I, pfmyo-c has a leucine zipper pattern within the head domain (43). Although protein expression of this kind of myosin has not been identified, it is possible that this kind of myosin may play a role in organelle transport in the parasite and/or act as nuclear DNA binding protein.

Development from trophozoite to schizont may require more kinds of myosin other than myosin II. At development from trophozoite to schizont stage, the surface area of the trophozoite now enlarges greatly, and PVM and TVN expand. Some of these configurations reach the underside of the erythrocyte membrane. Some of the proteins produce small knobs on the erythrocyte surface. Synthesis of the molecules needed for parasite multiplication, including DNA, start in the trophozoite stage. The parasite undergoes nuclear division to reach shcizont stage. During trophozoite to schizont stage, there is also an increase in endocytosis of small vaculoes. Myosin I has been found to be involved in endocytic and exocytic membrane traffic. (27). The key features of development from trophozoite to schizont stage is asexual replication and merozoite formation. Microtubules play a role in migration of chromosome into merozoite. Inhibitors of microtubule (Taxol and EpA) were found to prevent the formation of merozoites from the pinching off of the mother schizont during

merogony, but the migration and distribution of the rhoptries and micronemes appeared to be unaffected (63). There are evident of myosin in organelle transport such as myosin V, which is a fundamental component of organelle transport. Its possible cargoes are melanosomes, synaptic vesicles, vacuoles and mRNA. Data from DeRisi *Plasmodium falciparum* HB3 time course microarray of pfmyo-a, pfmyo-b and pfmyo-d mRNA expression showed that these mRNA start to be express at 35-36 h post invasion, which is the time for schizont development, and have the highest expression at 38-44 h post invasion then gradual decrease until 4-6 h post invasion of the next cycle (14). So these parasite myosins may play a role in parasite cytokinesis and/or migration and distribution of rhoptries and micronemes during merogony.

Development from schizont to ring stage may also require others kind of myosin than myosin II. Myosin II is found in erythrocyte and not in the parasite. Since erythrocytes are normally nonphagocytic, the effects of the inhibitors on *Plasmodium* invasion are likely to represent inhibitor disruption of parasite (not host cell) microfilaments. Invasion is three to four times faster than phagocytosis (occurring within 25 to 40 sec) and in characterized by parasite penetration into a tight-fitting vacuole formed by invagination of the plasma membrane. This is in contrast to phagocytosis of *Toxoplasma* involves membrane ruffling and the parasite is captured in a loose-fitting phagosome that forms over 2 to 4 min (64). In 1998, JC Pinder et al (21) found that BDM inhibits *P. falciparum* invasion from schizont to ring stage with IC_{50} of about 5 mM, which consistent with our data (IC_{50}=5.4 mM), and invasion starting with merozoite was decreased from 7.2 % to 1.2 % at presence of 12 mM BDM. The data in Figure15 give an additional knowledge from previous report and showed that decreasing of ring number is not only the inhibitory effect of BDM on merozoite invasion but also due to the inhibitory effect of BDM on schizont rupture. Thus, taken altogether, *P. falciparum* myosin is required for both schizont rupture and merzoite invasion. BDM also inhibits invasion of relative organism *Toxoplasma godii* at 20-40 mM (65). From data of *P. falciparum* myosin mRNA expression as described earlier, the highest expression occurs at 38-44 h post invasion then gradual decreases until 4-6 h post invasion of the next cycle. This consistent with immunofluorescence data from Pinder and her colleagues who found that Pfmyo-A is synthesized in schizont and vanishes after parasite enter the erythrocyte. The stage specificity of the

expression makes it highly probable that this myosin is the motor in the invasion mechanism (22). Although, only protein expression of Pfmyo-A has been reported in the parasite, but it is possible that Pfmyo-B and Pfmyo-D may play roles in parasite release and invasion.

5.4 Combination effect of the inhibitors on parasite growth.

As mentioned earlier, activation of myosin ATPase activity requires phosphorylation by myosin light chain kinase. In order to demonstrate that BDM, myosin ATPase inhibitor, and ML-7, MLCK inhibitor, have these modes of action within the parasite, the effects of a combination of the two drugs were determined. The expectation was that there should be a synergistic effect, i.e. the presence of sub-inhibitory concentrations of one drug should reduce the IC_{50} values of the other drug. Sub-inhibitory concentrations of BDM had no effect on the IC_{50} values of ML-7 (see Figure 23A) nor did sub-inhibitory concentrations of ML-7 had any effect on the IC_{50} values of BDM. This can be explained by the fact that as the concentrations of one drug used were too low to affect myosin function, it should not affect the inhibitory effects of the other drug. Although FIC of BDM was increased (≥ 2.5) in the presence of ML-7 (Figure 23B), these values are not significantly different from IC_{50} of BDM alone. In order to obtain more definitive information, a complete isobologram must be constructed.

CHAPTER 6
CONCLUSION

Malaria parasite invades and develops within the human host erythrocyte. It causes changes to the erythrocyte shape and deformability. Erythrocyte type II myosin controls the red cell biconcave shape; its activity is regulated by phosphorylation of the myosin light chain by myosin light chain kinase (MLCK) which then activates myosin ATPase activity. *P. falciparum* myosins have been reported to play a role in parasite invasion.

Investigations of the role of myosin-based contractile system of *P. falciparum* and host red cell during parasite growth within the erythrocyte, and in the invasion process, were conducted by using ML-7, a myosin light chain kinase inhibitor, and BDM, a myosin ATPase inhibitor.

Using ^{3}H-hypoxanthine incorporation assay, ML-7 and BDM inhibited growth of the parasite from ring to schizont stage with IC_{50} of 6.3±1.1 μM and 6.4±1.1 mM, respectively. The particular stages of development affected by these inhibitors were determined by counting parasitemia under a microscope. BDM could inhibit development at every stage (ring to trophozoite, trophozoite to schizont, and schizont to ring) at similar concentrations showing that myosin ATPase activity is required during all stages of malaria parasite intraerythrocytic growth and development, including the schizont rupture and merozoite invasion step. ML-7 inhibited development from ring to trophozoite stage at μM concentration, whereas development of trophozoite to schizont stage, and from schizont to ring stage (invasion step), required 10 fold more inhibitor. Thus, development of ring to trophozoite stage in parasite intraerythrocytic growth requires a ML-7-sensitive MLCK. Taken altogether, these finding indicated that development from ring to trophozoite may require myosin II function, while development from trophozoite to

schizont stage and development from schizont to ring stage may require more kinds of myosin other than myosin II.

In order to demonstrate that BDM, myosin ATPase inhibitor, and ML-7, MLCK inhibitor, have these modes of action within the parasite, the effects of a combination of the two drugs were determined. Sub-inhibitory concentrations of BDM had no effect on the IC_{50} values of ML-7 nor did sub-inhibitory concentrations of ML-7 had any effect on the IC_{50} values of BDM. This can be explained by the fact that as the concentrations of one drug used were too low to affect myosin function, it should not affect the inhibitory effects of the other drug.

REFERENCES

1. World Health Organization. World malaria situation in 1994. WHO Weekly Epidemiol Rec 1997; 36: 269-76.
2. World Health Organization. Malaria (the current situation). WHO division of control of tropical disease 1995.
3. World Health Organization. Vector control for malaria and other mosquito-borne disease. Geneva: WHO, 1995. WHO Tech Rep Ser. no. 857.
4. Butter D. Time to put malaria control on the global agenda. Nature 1997; 386: 535-8.
5. World Health Organization. World malaria situation 1990. Wld Hlth Statistist Quart 1992; 45: 257-66.
6. Bannister L, Mitchell G. The ins, outs and roundabouts of malaria. Trends Parasitol 2003; 19: 209-13.
7. Anders RF, Saul A. Malaria vaccines. Parasitol Today 2000; 16: 444-47.
8. Holder AA. Malaria vaccines. Proc Natl Acad Sci USA 1999; 96: 1167-9.
9. Lobo CA, Kumar N. Sexual Differentiation and Development in the Malaria Parasite. Parasitol Today 1998; 14: 146-50.
10. Wahlgren M, Perlmann P. Malaria Molecular and clinical Aspects. Harwood academic publishers. 1999.
11. Mota MM, Hafalla JC, Rodriguez A.Migration through host cells activates *Plasmodium* sporozoites for infection. Nat Med 2002; 8: 1318-2.
12. Sibley LD. Intracellular parasite invasion strategies. Science 2004; 304: 248-53.
13. Bannister LH, Hopkins JM, Fowler RE, Krishna S, et al. A brief illustrated guide to the ultrastructure of *Plasmodium falciparum* asexual blood stages. Parasitol Today 2000; 16: 427-33.
14. Bozdech Z, Llinas M, Pulliam BL, Wong ED, Zhu J, DeRisi JL. The transcriptome of intraerythrocytic developmental cycle of *Plasmodium falciparum*. PloS Biol 2003; 1: 85-99.

15. Wiser MF, Lanners HN, Bafford RA. Export of *Plasmodium* protein via a Novel secretory pathway. Parasitol Today 1999; 15: 194-8.
16. Cooke BM, Mohandas N, Coppel RL. The malarai-infected red blood cell: structural and functional changes. Adv Parasitol 2001; 50: 1-62.
17. Nagao E, Kaneko O, Dvorak JA. *Plasmodium falciparum*-Infected Erythrocytes: Qualitative and Quantitative Analyses of Parasite-Induced Knobs by Atomic Force Microscopy. J Struct Biol 2000; 130: 34-44.
18. Salmon BL, Oksman A, Goldberg DE. Malaria parasite exit from the host erythrocyte: A two-step process requiring extraerythrocytic proteolysis. PNAS 2001; 98: 271-6.
19. Cowman AF, Baldi DL, Healer J, Mills KE, O'Donnell RA, Reed MB, Triglia T, Wickham ME, Crabb BS. Functional analysis of protein involved in *Plasmodium falciparum* merozoite invasion of red blood cell. FEBS Lett 2000; 476: 84-8.
20. Pinder JC, Fowler RE, Bannister LH, Dluzewski AR, Mitchell GH. Motile systems in malaria merozoites: how is the red cell invaded?. Parasitol Today 2000; 16: 240-5.
21. Fowler RE, Fooks RE, Lavin Ff, Bannister LH, Mitchell GH. Microtubules in *Plasmodium falciparum* merozoites and their importance for invasion of erythrocyte. Parasitology 1998; 117: 425-33.
22. Pinder JC, Fowler RE, Dluzewski AR, Bannister LH, Lavin FM, Mitchell GH, Wilson RJM, Gratzer WB. Actomyosin motor in the merozoite of the malaria parasite, *Plasmodium falciparum*: implications for red cell invasion. J Cell Sci 1998; 111: 1831-9.
23. Sellers JR. Myosins: a diversity superfamily. Biochim Biophys Acta 2000; 1496: 3-22.
24. Thompson RF, Langford GM. Myosin superfamily evolutionary history. Anat Rec 2002; 268: 276-89.
25. Korn ED. Coevolution of head, neck, tail domains of myosin heavy chains. Proc Natl Acad Sci USA 2000; 97: 12559-64.
26. Cooper GM. The Cell: A molecular approach. 2 nd ed. Sinauer Associayes, Inc. Massachusetts; 2000. p. 421-63.

27. Mermall V, et al. unconventional myosins in cell movement, membrane traffic and signal transduction. Science 1998; 279: 527-33.
28. Wong AJ, Kiehart DP, Pollard TD. Myosin from Human erythrocytes. J Biol Chem 1985; 260: 46-9.
29. Fowler VM, Davis JQ, Bennett V. Human erythrocyte myosin: Identification and purification. J Cell Biol 1985; 100: 47-55.
30. Fowler VM. An actomyosin contractile mechanism for erythrocyte shape transformations. J Cell Biochem 1986; 31: 1-9.
31. Foder B, Scharff O. Decrease of apparent calmodulin affinity of erythrocyte (Ca^{2+} + Mg^{2+})-ATPase at low Ca2+ concentrations. Biochim Biophys Acta 1981; 649: 367-76.
32. der Terrossian E, Deprette C, Lebbar I, Cassoly R. Purification and characterization of erythrocyte caldesmon. Hypothesis for an actin-linked regulation of a contractile activity in the red blood cell membrane. Eur J Biochem 1994; 219: 503-11.
33. Knipper M, Zimmermann U, Kopschall I, Rohbock K, Jungleing S, Zenner H. Immunological identification of candidate proteins involved in regulating active shape changes of outer hair cells. Hearing Res 1995; 86: 100-10.
34. Cibert C, Pruliere G, Lacombe C, Deprette C, Cassoly R. Calculation of a Gap restoration in the membrane skeleton of the red blood cell: possible role for myosin II in local repair. Biophys J 1999; 76: 1153-65.
35. Pasternack GR, Racusen RH. Erythrocyte protein 4.1 binds and regulates myosin. Proc Natl Acad Sci USA 1989; 86: 9712-6.
36. Szent-Gyorgyi AG. Regulation of contraction by calcium binding myosins. Biophys Chem 1996; 59: 357-63.
37. Barylko B, Binns DD, Albanesi JP. Regulation of the enzymatic and motor activities of myosin I. Biochim Biophys Acta 2000; 1496: 23-35
38. Gallagher PJ, Herring BP, Stull JT. Myosin light chain kinases.J Muscle Res Cell Motil 1997 ; 18: 1-16.
39. de la Roche MA, Cote GP. Regulation of *Dictyostelium* myosin I and II. Biochim Biophys Acta. 2001; 1525: 245-61.

40. Morrissette NS, Sibley LD. Cytoskeleton of Apicomplexan Parasites. Microbiology and Molecular Biology Reviews 2002; 66: 21-38.
41. Heintzelmann MB and Schwartzman JD. Myosin diversity in apicomplexa. J Parasitol 2001; 87: 429-32.
42. Matuschewski K, Mota MM, Pinder JC, Nussenzweig V, Kappe SH. Identification of the class XIV myosins Pb-MyoA and Py-MyoA and expression in *Plasmodium* sporozoites. Mol Biochem Parasitol 2001; 112: 157-61.
43. Lew AE, Dluzewski AR, Johnson AM, Pinder JC. Myosins of *Babesia bovis*: Molecular characterization, erythrocyte invasion, and phylogeny. Cell Motil Cytoskeleton 2002; 52: 202-20.
44. Saitoh M, Ishikawa T, Matsushima S, Naka M, Hidaka H. Selective Inhibition of Catalytic Activity of Smooth Muscle Myosin Light Chain Kinase. J Biol Chem 1987; 262: 7796-801.
45. Cramer LP, Mitchison TJ. Myosin is involved in postmitotic cell spreading. J Cell Biol 1995; 131: 179-89.
46. Herrmann C, Wray J, Travers F, Barman T. Effect of 2,3-Butanedione monxime on myosin and myofibrillar ATPases. An example of an uncompetitive inhibtor. Biochemistry 1992; 31: 12227-32.
47. Thaitong S, Beale GH, Chutmongkonkul M. Susceptibility of *Plasmodium falciparum* to five drugs: an in vitro study of isolates mainly from Thailand. Trans R Soc Trop Med Hyg 1983; 77: 228-31.
48. Trager W, Jensen JB. Human malaria parasites in continuous culture. Science 1976; 193: 673-75.
49. Jensen JB, Trager W. *Plasmodium falciparum* in culture: use of outdated erythrocytes and description of the candle jar method. J Parasitol 1977; 63: 883-6.
50. Lambros C, Vanderberg JP. Synchronization of *Plasmodium falciparum* erythrocytic stages in culture. J Parasitol 1979; 65: 418-20.
51. Khusmith S, Tapchaisri P, Tharavanij S, Bunnag D. Antigenic diversity of *Plasmodium vivax* and their geographic distribution in Thailand. Southeast Asian J Trop Med Public Health 1998; 29: 512-8.

52. Desjardins RE, Canfield CJ, Haynes JD, Chulay JD. Quantitative assessment of antimalarial activity in vitro by a semiautomated microdilution technique. Antimicrob Agents Chemother 1979; 16: 710-8.

53. Chukay JD, Haynes JD, Diggs CL. *Plasmodium falciparum*: assessment of in vitro growth by [^{3}H]hypoxanthine incorporation. Exp Parasitol 1983; 55: 138-46.

54. Manandhar MSP, Dyke KV. Detailed purine salvage metabolism in and out the free malaria parasite. Exp Parasitol 1975; 37: 138-46.

55. Sellin LC, McArdle JJ. Multiple effects of 2,3-Butanedione monoxime. Pharmacology&Toxicology 1994; 74: 305-13.

56. Urwyler N, Eggli P, Keller HU. Effect of the myosin inhibitor 2,3-butanedione monoxime (BDM) on cell shape, locomotion and fluid pinocytosis in human polymorphonuclear leucocytes. Cell Biol Int. 2000; 24: 863-70.

57. Duran JM, Valderrama F, Castel S, Magdalena J, Tomas M, Hosoya H, Renau-Piqueras J, Malhotra V, Egea G. Myosin Motors and not actin comets are mediators of the actin-based Golgi-to-Endoplasmic Reticulum protein transport. Mol Biol Cell 2003; 14: 445-59.

58. Phillips RM, Altschuld RA. 2,3-butanedione 2-monoxime (BDM) induces calcium release from canine cardiac sarcoplasmic reticulum. Biochem Biophys Res Commun 1996; 229: 154-57.

59. Kaneko K, Satoh K, Masamune A, Satoh A, Shimosegawa T. Myosin light chain kinase inhibitors can block invasion and adhesion of human pancreatic cancer cell line. Pancreas 2002; 24: 34-41

60. Tohtong R, K Phattarasakul, A Jiraviriyakul and T Sutthiphongchai. Dependence of metastatic cancer cell invasion on MLCK-catalyzed phosphorylation of myosin regulation of myosin regulation light chain. Prostate Cancer and Prostatic Dis 2003; 6: 212-16.

61. Douki JB, Sterkers Y, Lepolard C, Traore B, Costa FT, Scherf A, Gysin J. Adhesion of normal and *Plasmodium falciparum* ring-infected erythroyctes to endothelial cells and the placenta involves the rhoptry-derived ring surface protein-2. Blood 2003; 101: 5025-32.

62. Taraschi TF, O'Donnell M, Martinez S, Schneider T, Trelka D, Fowler VM, Tilley L, Moriyama Y. Generation of an erythrocyte vesicle transport system by *Plasmodium falciparum* malaria parasites. Blood 2003; 102: 3420-26.

63. Taraschi TF, Trelka D, Schneider T, Matthews I. *Plasmodium falciparum*: Characterization of organelle migration during merozite morphogenesis in asexual malaria infections. Exp Parasitol 1998; 88: 184-93.

64. Morisaki JH, Heuser JE, Sibley LD. Invasion of *Toxoplasma gondii* occurs by active penetration of the host cell. J Cell Sci 1995; 108: 2457-64.

65. Dobrowolski JM, Carruthers VB, Sibley LD. Participation of myosin in gliding motility and host cell invasion by *Toxoplasma gondii*. Mol Microbiol 1997; 26: 163-73.

APPENDIX

APPENDIX

1. Giema's stain

Stain stock solution

Giemsa powder (BDH,U.K.)	0.6	g
Glycerol	50	ml
Absolute methanol, acetone free	50	ml

A small amount of Giemsa powder was placed in a mortar with a small amount of glycerol. The dye powder and glycerol were ground thoroughly until they all mixed together. The glycerol-dye mixture was incubated in water bath set at 55-60 ^{o}C for 6-8 h with periodic shaking. After cooling to room temperature, 50 ml methanol was added and the dye was kept at 37 ^{o}C for 2 weeks in stopper bottle. The dye was then filtered and stored in dark bottle.

Phosphate buffer (pH 7.2)

0.067 M Na_2HPO_4	9.47	g/L
0.067 M KH_2PO_4	9.38	g/L

2. Staining

A smear was fixed for 1 min in acetone-free methanol and allowed to air-dry. The smear was then soaked with a solution containing a ratio of Giemsa's stain: phosphate buffer pH 7.2 of 10 : 90 (or 10% v/v) about 10 min then rinsed with tap water. The air-dried slide was examined under a microscope with 100 x magnification oil-immersion lens. The percent parasitemia was determined by the percentage of the infected erythrocytes from a total of 1,000 erythrocytes.

BIOGRAPHY

NAME	Miss Usawadee Sakulkhu
DATE OF BIRTH	25 June1979
PLACE OF BIRTH	Udonthani, Thailand
INSTITUTIONS ATTENDED	Khon Kean University, 1996-1999: Bachelor of Science (Biochemistry)
	Mahidol University, 2000-2003: Master of Science (Biochemistry)
HOME ADDRESS	568/14 Assawamit Road, Magkheang District, Amper Muang, Udonthani Province, Thailand